Clinical Studies of Exposure to Ultrafine Particles

Final Report 05-11
November 2005

New York State
Energy Research and
Development Authority

NYSERDA

The New York State Energy Research and Development Authority (NYSERDA) is a public benefit corporation created in 1975 by the New York State Legislature. NYSERDA's responsibilities include:

- Conducting a multifaceted energy and environmental research and development program to meet New York State's diverse economic needs.
- Administering the **New York Energy $mart℠** program, a Statewide public benefit R&D, energy efficiency, and environmental protection program.
- Making energy more affordable for residential and low-income households.
- Helping industries, schools, hospitals, municipalities, not-for-profits, and the residential sector, including low-income residents, implement energy-efficiency measures.
- Providing objective, credible, and useful energy analysis and planning to guide decisions made by major energy stakeholders in the private and public sectors.
- Managing the Western New York Nuclear Service Center at West Valley, including: (1) overseeing the State's interests and share of costs at the West Valley Demonstration Project, a federal/State radioactive waste clean-up effort, and (2) managing wastes and maintaining facilities at the shut-down State-Licensed Disposal Area.
- Coordinating the State's activities on energy emergencies and nuclear regulatory matters, and monitoring low-level radioactive waste generation and management in the State.
- Financing energy-related projects, reducing costs for ratepayers.

NYSERDA administers the **New York Energy $mart℠** program, which is designed to support certain public benefit programs during the transition to a more competitive electricity market. Some 2,700 projects in 40 programs are funded by a charge on the electricity transmitted and distributed by the State's investor-owned utilities. The **New York Energy $mart℠** program provides energy efficiency services, including those directed at the low-income sector, research and development, and environmental protection activities.

NYSERDA derives its basic research revenues from an assessment on the intrastate sales of New York State's investor-owned electric and gas utilities, and voluntary annual contributions by the New York Power Authority and the Long Island Power Authority. Additional research dollars come from limited corporate funds. Some 400 NYSERDA research projects help the State's businesses and municipalities with their energy and environmental problems. Since 1990, NYSERDA has successfully developed and brought into use more than 170 innovative, energy-efficient, and environmentally beneficial products, processes, and services. These contributions to the State's economic growth and environmental protection are made at a cost of about $.70 per New York resident per year.

Federally funded, the Energy Efficiency Services program is working with more than 540 businesses, schools, and municipalities to identify existing technologies and equipment to reduce their energy costs.

For more information, contact the Communications unit, NYSERDA, 17 Columbia Circle, Albany, New York 12203-6399; toll-free 1-866-NYSERDA, locally (518) 862-1090, ext. 3250; or on the web at www.nyserda.org

State of New York
George E. Pataki
Governor

Energy Research and Development Authority
Vincent A. DeIorio, Esq., Chairman
Peter R. Smith, President and Chief Executive Officer

Clinical Studies of Exposure to Ultrafine Particles

Final Report

Prepared for the

New York State Energy Research and Development Authority

Albany, NY
www.nyserda.org

Ellen Burkhard
Project Manager

Prepared by:

The University of Rochester

Mark J. Utell
Mark W. Frampton
Co-Principal investigators

NYSERDA
Report 05-11

NYSERDA 4913

November 2005

NOTICE

This report was prepared by the University of Rochester in the course of performing work contracted for and sponsored by the New York State Energy Research and Development Authority (hereafter the "Sponsor"). The opinions expressed in this report do not necessarily reflect those of the Sponsor or the State of New York, and reference to any specific product, service, process, or method does not constitute an implied or expressed recommendation or endorsement of it. Further, the Sponsor and the State of New York make no warranties or representations, expressed or implied, as to the fitness for particular purpose or merchantability of any product, apparatus, or service, or the usefulness, completeness, or accuracy of any processes, methods, or other information contained, described, disclosed, or referred to in this report. The Sponsor, the State of New York, and the contractor make no representation that the use of any product, apparatus, process, method, or other information will not infringe privately owned rights and will assume no liability for any loss, injury, or damage resulting from, or occurring in connection with, the use of information contained, described, disclosed, or referred to in this report.

ABSTRACT

Increased levels of particulate air pollution are associated with increased cardiovascular and respiratory mortality and morbidity. Ultrafine particles (UFP; diameter < 100 nm, or 0.1 μm) may contribute to these adverse effects because of their potential to induce pulmonary inflammation, high-predicted pulmonary deposition, large surface area, and ability to enter the pulmonary interstitium and vascular space. Our objective was to initiate clinical studies of exposure to ultrafine particles in healthy human subjects. These studies examined the role of ultrafine particle exposure in 1) the induction of airway inflammation; 2) leukocyte and endothelial adhesion molecule expression in the blood; 3) alterations in blood coagulability; and 4) alterations in cardiac electrical activity. Furthermore, these studies examined the effects of exercise on ultrafine particle deposition in the lung, pulmonary function responses, the acute-phase inflammatory response, and cardiac repolarization. Healthy subjects inhaled filtered air and freshly generated elemental carbon particles (count median diameter ~25 nm, geometric standard deviation ~1.6) for 2 hours, in three separate protocols: 10 $\mu g/m^3$ at rest, 10 and 25 $\mu g/m^3$ with exercise, and 50 $\mu g/m^3$ with exercise. Prior to and at intervals after each exposure, we assessed symptoms, pulmonary function, blood markers of inflammation and coagulation, and airway nitric oxide (NO) production. Sputum inflammatory cells were assessed 21 hours after exposure. Continuous 12-lead electrocardiography recordings were analyzed for changes in heart rate variability and repolarization. The diffusing capacity for carbon monoxide was measured 21 hours after exposure in the 50 $\mu g/m^3$ exposure protocol.

We found that the fractional deposition of UFP at rest was 0.66 ± 0.12 (mean ± SD) by particle number, confirming the high deposition predicted by models. Deposition further increased during exercise (0.83 ± 0.04). During the 10 $\mu g/m^3$ rest protocol, there was no convincing effect for any outcome measure. Breathing 25 $\mu g/m^3$ UFP with exercise was associated with reductions in blood monocytes and activation of T lymphocytes in healthy females, and 50 $\mu g/m^3$ similarly activated T lymphocytes. Monocyte expression of intracellular adhesion molecule-1 (ICAM-1, CD54) was reduced in a concentration-related manner in the 10 and 25 $\mu g/m^3$ exposures with intermittent exercise and also at 50 $\mu g/m^3$ UFP concentration in males. Electrocardiogram (ECG) analyses showed repolarization changes with exposures to 10 and 25 $\mu g/m^3$, but not with 50 $\mu g/m^3$. The diffusing capacity decreased 21 hours after exposure to 50 $\mu g/m^3$.

The observed subtle changes in leukocyte subsets and adhesion molecule expression are consistent with effect on vascular endothelial function. The reduction in diffusing capacity 21 hours after exposure to UFP may also reflect an effect on the pulmonary vascular system. If confirmed, the findings that inhalation of UFP has cardiovascular effects would be highly relevant to our understanding of particle-induced health effects.

PREFACE

The New York State Energy Research and Development Authority is pleased to publish "Clinical Studies of Exposure to Ultrafine Particles." The report was prepared by the principal investigator, Mark J. Utell, M.D. of the University of Rochester Medical Center.

This study was conducted at the University of Rochester Medical Center, a U.S. Environmental Protection Agency Particulate Matter Health Center. The study investigated the pulmonary and cardiac effects from inhaling ultra-fine particles (UFP) in healthy subjects. The study was supported because little is known about the specific mechanism by which particulate matter and/or its components cause health effects. Ambient UFP are regarded as important to respiratory health because they are biologically reactive, have high number concentration, and have high deposition efficiency in the pulmonary region. An additional study by the University of Rochester Medical Center will investigate the effect of ambient UFP on a susceptible population living in Rochester, NY. The temporal variation of UFP in this city was characterized in a previous NYSERDA-funded project by Professor Phil Hopke of Clarkson University. Dr. Hopke's work showed periods of high UFP number concentration, diurnal variations, and identified particle nucleation and growth events. (See http://www.nyserda.org/programs/Environment/EMEP/ for more information.)

The work was funded by the New York Energy $mart[SM] Environmental Monitoring, Evaluation, and Protection (EMEP) Program.

TABLE OF CONTENTS

Section Page

EXECUTIVE SUMMARY S-1

1 INTRODUCTION 1-1

2 DEVELOPMENT OF AN ULTRAFINE PARTICLE EXPOSURE SYSTEM 2-1
System Design 2-1
Particle Generation 2-3
Particle Characterization 2-4
Particle Composition 2-5
System Losses 2-6
Respiratory Measurements 2-7

3 EXPOSURE PROTOCOL AND PARTICLE DEPOSITION 3-1

4 BIOLOGIC ENDPOINTS 4-1
Pulmonary Function 4-1
Airway Nitric Oxide 4-1
Blood Markers of Coagulation and Inflammation 4-1
Blood Leukocyte Immunofluorescence Analysis 4-2
Septum Induction 4-3
Cardiac Monitoring 4-3
Calculation of Particle Deposition 4-3
Statistical Methods 4-4

5 RESULTS 5-1
Particle Concentrations in the Research Environment 5-1
Particle Deposition (Task 2) 5-1
Biological Effects (Tasks 3 and 4) 5-6
Exposures at Rest 5-6
Exposures with Exercise 5-6
Exposure to 10 and 25 $\mu g/m^3$ UFP 5-6
Exposure to 50 $\mu g/m^3$ UFP 5-12

6 DISCUSSION 6-1

GLOSSARY R-1
RELATED PUBLICATIONS R-2
REFERENCES R-4

FIGURES AND TABLES

Figure Page

S-1 The ultrafine particle exposure system S-2

S-2 Particle number deposition fraction and total particle deposition at rest and during exercise S-3

S-3 Change in pulmonary diffusing capacity (DL_{CO}) before and after exposure to filtered air vs. 50 μg/m^3 UFP S-4

2-1 Ultrafine particle generation and exposure system 2-2

2-2 Size distribution, by number, of ultrafine carbon particles generated for inhalation 2-5

3-1 Experimental protocol for the clinical studies 3-1

5-1 Typical results of real-time monitoring of mass and number concentrations during an exposure. 5-3

5-2 Hemoglobin-oxygen saturation by pulse oximetry in 6 females exposed to air and 10 and 25 μg/m^3 UFP 5-7

5-3 Expression of intercellular adhesion molecule-1 (ICAM-1, CD54) on blood monocytes, by multiparameter flow cytometry 5-8

5-4 Percentage of blood monocytes from the leukocyte differential count 5-8

5-5 Expression of CD25 on blood lymphocytes, by multiparameter flow cytometry 5-9

5-6 Changes in high-frequency component of heart rate variability 5-10

5-7 Changes in the QT interval (uncorrected) on the ECG recording 5-10

5-8 Changes in the QT interval, using Bazette's correction for heart rate 5-11

5-9 Changes in T-wave amplitude on the ECG recording 5-11

5-10 Change in monocyte expression of CD18 after exposure to 50 μg/m^3 carbon UFP 5-12

5-11 Change in DL_{CO} before and after exposure to filtered air vs. 50 μg/m^3 UFP 5-13

5-12 Change in alveolar airway NO parameters after exposure to filtered air versus UFP 5-14

5-13 Change in cardiac normal-to-normal beat interval with exposure to air versus 50 μg/m^3 UFP 5-15

5-14 Change in low-frequency heart rate variability expressed as normalized units..... 5-16

Table Page

S-1 Numbers and surface area of particles of unit density of different sizes at a mass concentration of 10 μg/m^3 ..... S-2

2-1 Equipment for the ultrafine particle exposure facility..... 2-3

2-2 Particle losses in the exposure system..... 2-7

5-1 Subject demographics 5-3

5-2 Breathing parameters 5-4

5-3 Deposition fraction by particle size in 12 healthy subjects at rest (Series 1) 5-4

5-4 Deposition fraction (DF) in 7 healthy subjects at rest and exercise (Series 2)..... 5-5

EXECUTIVE SUMMARY

In 1997, the U.S. Environmental Protection Agency (EPA) set a new mass-based National Ambient Air Quality Standard (NAAQS) for airborne particles smaller than 2.5 microns in diameter, called $PM_{2.5}$. Currently, the New York State Department of Environmental Conservation (NYS DEC) is conducting a three-year monitoring program to identify areas in New York State that may not meet the mass-based $PM_{2.5}$ NAAQS.

Airborne particulate matter is a broad class of materials of varying composition and sizes that are transported in the air as solid particles or liquid droplets. Airborne particles are emitted from a variety of natural processes and human activities, including fossil-fuel combustion, forest fires, wind erosion, agricultural practices, industrial manufacturing, and construction processes. The particles can be emitted directly into the atmosphere (primary particles) or formed in the atmosphere from precursor gases (e.g., sulfur dioxide, nitrogen oxides, ammonia, and volatile organic compounds). Ultrafine particles (UFPs) are extremely small particles, less than 0.1 micron in diameter. These particles are primarily generated from combustion processes, including stationary fossil-fueled electric-power generation, industrial processes, boilers, and car and truck engines.

While a variety of studies have shown a correlation between elevated concentrations of ambient particulate matter and adverse health effects, the exact mechanisms and chemical components responsible for the biological activity are not fully understood. Consequently, as EPA and the States proceed with the early phases of implementation of the mass-based $PM_{2.5}$ NAAQS, numerous parallel research projects are underway to better understand which components in the PM mixture are responsible for the adverse health effects. Several hypotheses have been proposed, and several components/characteristics of PM have been targeted for exploration, including the UFP fraction of PM. Recently, findings from a panel study of the elderly in Fresno, California by investigators at the U.S. EPA showed a strong indication that UFP are having a significant impact on heart rate variability. Ultrafine particles may induce vascular effects by their ability to evade macrophage phagocytosis via the scavenger receptor, and to enter alveolar epithelial cells and even capillary blood. This project explores the hypothesis that UFP are a key culprit responsible for adverse health effects associated with fine particles. The results could have a significant impact on national regulatory control strategies and future ambient air quality standards.

Ambient UFP are important with regard to respiratory health for several reasons. They are biologically more reactive than larger particles and elicit effects at low mass concentrations. At the same ambient mass concentration, UFPs have a much higher concentration in terms of the number of particles and surface area than fine particles (see Table S-1). They also show high deposition efficiency in the pulmonary region, since the probability of deposition by diffusion increases as particle size decreases. UFP exhibit a higher

propensity to rapidly reach the systemic circulation; they may therefore be linked to the cardiovascular effects attributed to the fine particle fraction.

Table S-1: Numbers and Surface Area of Particles of Unit Density of Different Sizes at a Mass Concentration of 10 μg/m^3

Particle Diameter μm	Particle Number 1/cm^3	Particle Surface Area μm^2/cm^3
0.02	2,400,000	3016
0.1	19,100	600
0.5	153	120
1.0	19	60
2.5	1.2	24

The project initiated clinical studies of exposure to UFP in healthy human subjects. Our hypothesis was that the increases in morbidity and mortality that are associated with ambient air pollution are related to increased airway inflammation in susceptible individuals. In addition, we proposed that UFP exposure through ambient air alters pulmonary and vascular function, activation of circulating white blood cells (leukocytes), and the recovery of the heart from a beat (cardiac repolarization).

We developed an UFP exposure system and a clinical protocol incorporating measurements of particle deposition that were used in three studies on UFP inhalation. The three protocols studied subjects with healthy, normal lung function. In the first study, 12 subjects at rest were exposed to 10 micrograms per cubic meter (μg/m^3) UFP and filtered air for two hours. In the second, each of 12 subjects underwent three exposures of air, 10 μg/m^3, and 25 μg/m^3 of carbon UFP for two hours, with intermittent exercise on a bicycle ergometer. In the third set of clinical studies, 16 subjects were exposed to ultrafine carbon particles at a concentration of 50 μg/m^3, again with intermittent exercise. This higher concentration reflects approximately twice the high-ambient concentrations found in Rochester, NY or the surrounding roadways.

In the exposures, ultrafine carbon particles were generated and diluted with filtered air, breathed by the subjects through a mouthpiece, then passed though one-way rebreathing valves (see Figure S-1). Exhaled particles and excess aerosol were removed through the exhaust system. Several exposure factors were monitored in real time through the mouthpiece exposure system. Particle mass concentrations, number concentrations, size distributions, and system losses were

Figure S-1. The ultrafine particle exposure system. The design incorporated a bicycle to examine the effects of UFP exposure during exercise.

determined. UFP deposition in the study subjects was measured by calculating the number of particles going in through the mouthpiece and the number coming out.

Using a detailed evaluation protocol, we assessed symptoms, pulmonary function, blood markers of inflammation and coagulation, and airway nitric oxide production prior to and at intervals after each exposure. Sputum inflammatory cells were assessed 21 hours after exposure. Continuous 12-lead electrocardiography recordings were analyzed for changes in heart rate variability and repolarization. In addition, the diffusing capacity for carbon monoxide (DL_{CO}) was measured 21 hours post-exposure in the 50 $\mu g/m^3$ exposure protocol.

The studies show that UFP inhalation by healthy subjects has a number of cardiovascular, rather than pulmonary, effects to which women may be more susceptible. These may be persistent or delayed, lasting for at least 21 hours after exposure. The project found:

- A high pulmonary deposition rate that increased with exercise (see Figure S-2). As expected, the smallest particles had the highest deposition rate. We found that the fractional deposition of UFP at rest was 0.66 ± 0.12 (mean ± SD) by particle number, confirming the high deposition predicted by models. Deposition further increased during exercise (0.83 ± 0.04). No gender difference was found in terms of deposition.

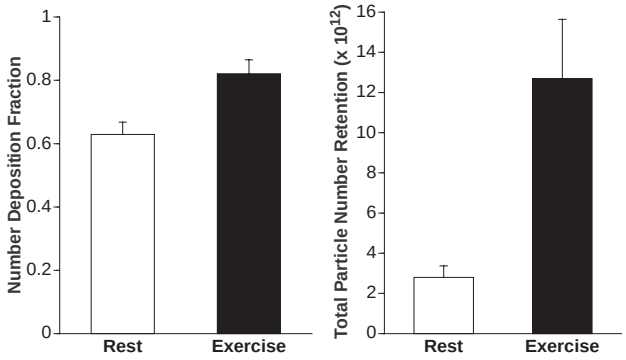

Figure S-2. Particle number deposition fraction and total particle deposition at rest and during exercise. Left panel shows the DF breathing at rest and during exercise. Right panel shows the calculated total particle deposition for subjects completing both rest and exercise exposures to 25 $\mu g/m^3$.

- No significant physiological changes in response to breathing 10 $\mu g/m^3$ UFP at rest. Also, we observed no evidence for airway inflammation or irritant effects or an early immune system response at 10, 25 or 50 $\mu g/m^3$ with intermittent exercise.

- Signs of alterations in cardiac repolarization (QT interval) with exposures to 10 and 25 $\mu g/m^3$, but not with 50 $\mu g/m^3$. The change observed during exercise was more pronounced with UFP exposure than with pure air, and remained in effect for several hours after UFP exposure, but not after pure air exposure. While the changes are small, they would nevertheless affect the mechanism of the heart, possibly leading to arrhythmia in people with underlying cardiac disease.

- A number of effects on circulating leukocytes, such as a reduction in the percentage of blood monocytes in females that were greatest 21 hours after exposure.
- Effects consistent with changes in blood vessel walls and how leukocytes move through the blood vessels.
- A reduction in the diffusing capacity of the lung for carbon monoxide 21 hours after exposure to carbon UFP at 50 μg/m^3 (see Figure S-3). We observed a decrease in blood oxygen saturation in females after exposure to 25 μg/m^3 UFPs.

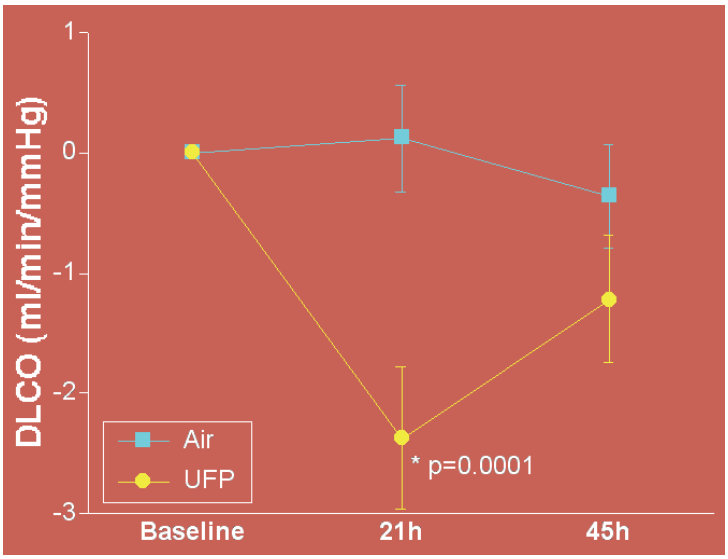

Figure S-3. Change in pulmonary diffusing capacity (DL_{CO}) before and after exposure to filtered air vs. 50 μg/m^3 UFP. There was a significant decline in DL_{CO} 21 hours after exposure to 50 μg/m^3 UFP. This difference resolved when the measurement was repeated 45 hours after exposure.

To briefly summarize the clinical findings, inhalation of carbon UFP at concentrations up to 50 μg/m^3 caused no symptoms, changes in lung function, or evidence for airway inflammation in healthy subjects. Blood leukocyte subsets and adhesion molecules expression did reveal changes consistent with alteration of vascular endothelial function. We also found effects on the diffusing capacity, which decreases significantly 21 hours post-exposure to UFP; the diffusing capacity is dependent on pulmonary capillary blood volume and also reflects effects on the pulmonary vascular system. Finally, we found effects on heart rate variability and on cardiac repolarization in healthy subjects.

While the particles generated for these studies from elemental carbon are relatively inert compared to UFP in ambient air, this research suggests that exposure to even these relatively benign particles at very low

mass concentrations during exercise has sub-clinical effects on blood flow to the lungs, circulating leukocytes, and cardiac repolarization in healthy subjects. If confirmed, the findings that inhalation of UFP have cardiovascular effects would be highly relevant to our understanding of particle-induced health effects. Furthermore, they would provide the most convincing support to date for current hypotheses about the health threats posed by UFP. The adverse health effects of UFPs raise the question of whether mass-based NAAQS are adequately protective of human health. While current $PM_{2.5}$ standards address mass concentrations of particulate matter in ambient air, a small mass concentration of particulate matter can mean very high number concentrations of UFP, which are 1–3 orders of magnitude smaller than fine particles. In addition, a decrease in the fine particle concentration in ambient air may lead to higher amounts of free-floating UFPs, as a key removal mechanism for UFP is their coagulation on fine particles. The results of further assessments of the cardiovascular and pulmonary effects of UFP may necessitate reconsideration of the regulatory regime for $PM_{2.5}$.

In summary, these data demonstrate that brief exposures to carbon UFP concentrations ranging from 10-50 $\mu g/m^3$ cause a range of cardiopulmonary responses. The effects were small but the low concentrations and brief exposures may not have been adequate to provoke large or sustained effects in healthy volunteers. Furthermore, with our findings indicating possible effects of carbon UFP on vascular endothelium, an important next step is to examine these processes in individuals with vascular disease risk factors or established cardiovascular disease. Our future studies will address cardiopulmonary responses to UFP using several different approaches: 1) we have extended our studies with carbon UFP to diabetics, a population with pre-existing vascular disease; 2) we plan to initiate studies with concentrated ambient (CAPs) UFP since the carbon UFP do not contain many of the constituents of outdoor UFP which are believed to be responsible for the adverse health effects, such as metals and organic species; and 3) finally, we have initiated studies to look at effects of inhaling ambient UFP in a group of patients with coronary artery disease who are actively participating in an exercise program in a Cardiac Rehabilitation facility. Further clinical studies are needed to confirm our findings to date, determine their relationship to particulate matter size and composition, and investigate their mechanisms.

Section 1

INTRODUCTION

We hypothesized that the increases in morbidity and mortality associated with ambient air pollution are related to exacerbation of airway inflammation in susceptible individuals. Further, we proposed that exposure to ultrafine particles (UFP; diameter < 100 nm, or 0.1 μm) in the ambient air enhances airway inflammation, is accompanied by changes in adhesion molecule expression by endothelial cells and circulating leukocytes, and is accompanied by transient increases in circulating acute-phase proteins and blood coagulability. Recently, investigators have expressed concern that ultrafine particles, because of their ability to rapidly enter the systemic circulation, might also be linked to the cardiovascular effects attributed to the fine particle fraction. Understanding the health effects of exposure to ultrafine particles is particularly important for determining risks associated with particulate matter (PM) air pollution and the potential effectiveness of control efforts in New York State.

We suggest that ambient UFP are important with regard to respiratory health effects, for several reasons:

1) UFP are biologically more reactive than larger particles and elicit effects at low concentrations.

2) UFP at the same mass concentration in the air have a much higher number concentration and surface area than larger particles. For example, to achieve a low airborne concentration of 10 $\mu g/m^3$, 2.4 x 10^6 ultrafine 20-nm particles/cm^3 are needed; in contrast, only one 2.5-μm particle/cm^3 is needed to reach the same concentration (1).

3) Inhaled singlet UFP have a very high deposition efficiency in the pulmonary region. For example, 20-nm particles have about 50% deposition efficiency (1).

4) UFP have a high propensity to penetrate the epithelium and reach interstitial sites and the systemic circulation (2).

Our studies use pure, laboratory-generated ultrafine carbon particles, analogous to some combustion emissions, and do not test the role of chemical composition. These studies are the first to assess health effects of exposure to UFP in humans.

Clinical studies are an important approach in understanding the mechanisms by which criteria air pollutants cause effects, and have played a critical role in the regulatory process and the setting of National Ambient Air Quality Standards. Our objective was to initiate clinical studies of exposure to ultrafine particles in healthy human subjects. We examined the role of ultrafine particle exposure in 1) the induction of airway inflammation; 2) leukocyte and endothelial adhesion molecule expression in the blood; 3) alterations in

blood coagulability; and 4) alterations in cardiac electrical activity. Furthermore, we examined the effects of exercise on ultrafine particle deposition in the lung, pulmonary function responses, the acute-phase inflammatory response, and cardiac repolarization.

The UFP number concentrations used in these studies are higher than UFP background concentrations but are relevant to episodic levels seen in specific situations. Ultrafine particles are always present in ambient air, with background urban levels in the range of 40–50,000 particles/cm^3, or estimated mass concentrations of 3–4 $\mu g/m^3$ (38). Continuous monitoring by our group in Rochester, New York, of UFP number and size between July 17, 2004, and July 25, 2005, revealed a maximum daily mean concentration on January 28, 2005. The mean number concentration was 2.55×10^4 particles/cm^3. The mass concentrations were calculated by assuming spherical particles with a density of 1.5 g/cm^3. The mean mass concentration of particles < 0.1 µm for this day was 2.45 $\mu g/m^3$, the maximum mass value of < 0.10 µm particles was 6.25 $\mu g/m^3$, and the average $PM_{2.5}$ for this day was 11.23 $\mu g/m^3$ (4; Dr. P. Hopke, personal communication). In Germany, episodic increases in UFP have been documented to 300,000 particles/cm^3, or estimated ~50 $\mu g/m^3$ of UFP as an hourly average (5, 6). Particle numbers inside a vehicle on a major highway reached 10^7 particles/cm^3, approximately 20 $\mu g/m^3$ (7). In recent studies that exposed caged rats to UFP on a highway in New York State, the daily average number concentration in the control (filtered air) chamber was $0.01–0.12 \times 10^5$ particles/cm^3. The incoming sampled air had a number concentration of $1.95–5.62 \times 10^5$ particles/cm^3. No direct measurements of mass concentration were made, but it was estimated to be 37–106 $\mu g/m^3$ (8). In a second truck on-road study performed by our group in New York State, the average concentrations of UFP were $1.6–4.3 \times 10^6/cm^3$ in the plume (9).

An interim final report submitted in March 2003 addressed four specific tasks: 1) develop an exposure system for clinical studies of ultrafine carbon particles; 2) develop a clinical protocol that includes rest and intermittent exercise at concentrations of 10 and 25 $\mu g/m^3$ and incorporates measurements of particle deposition; 3) determine the effects of UFP on airway inflammation, on the acute-phase response, and on coagulation factors at rest and under intermittent exercise; and 4) determine the effects of UFP on heart rate variability and repolarization at rest and with exercise.

In our prior report, we presented evidence that exposure to concentrations of 10 and 25 $\mu g/m^3$of carbonaceous UFP induced small alterations in blood oxygenation, in circulating monocytes and lymphocytes, and in cardiac repolarization. Some of these effects appeared to differ by sex, with female subjects showing increased susceptibility compared with males. Although these effects were not likely to be clinically important in healthy subjects, the fact that there were changes at all in healthy subjects was quite striking, and it was consistent with the hypothesis that these particles have the potential to elicit cardiovascular effects.

We therefore undertook an additional study designed to confirm and extend our initial observations in a larger group of healthy men and women, using a higher concentration of 50 $\mu g/m^3$, which is approximately twice as high as ambient concentrations found in Rochester, New York, and the surrounding roadways. We hypothesized that inhalation of UFP alters pulmonary vascular function, circulating leukocyte activation, and cardiac repolarization. In the supplemental study, we had two objectives: 1) to perform a human clinical inhalation study of randomized exposure to either filtered air or carbonaceous UFP, 50 $\mu g/m^3$ for 2 hours; and 2) to measure UFP effects on cardiac electrical activity, circulating leukocyte activation, and blood oxygenation. This report includes the protocol for the 50 $\mu g/m^3$ exposure, the new findings from this study, and an integrated, comprehensive summary looking across the findings from the 10, 25, and 50 $\mu g/m^3$ exposures.

Section 2

DEVELOPMENT OF AN ULTRAFINE PARTICLE EXPOSURE SYSTEM (TASK 1)

Our objectives in designing an exposure system for clinical studies of ultrafine particles (UFP) were as follows: 1) allow short-term controlled exposures to particles less than 100 nm; 2) measure respiratory tract deposition of UFP both at rest and with exercise; and 3) monitor changes in respiratory pattern and minute ventilation during exposure. A mouthpiece system best met these needs. Although whole-chamber or face-mask exposures would better simulate natural oral-nasal breathing, quantitative deposition measurements are more difficult with these exposure modes.

There are several requirements to meet the above objectives. First, particles must be generated in real time during exposure to minimize agglomeration and diffusive losses. Second, simultaneous measurements of particle number, mass, and size distribution are needed to characterize inhaled UFP. Third, determinations of particle characteristics are required on both the expiratory and the inspiratory side of the subject to determine deposition. Fourth, sufficient UFP aerosol must be provided to meet the range of inspiratory flow demands.

SYSTEM DESIGN

The design is a one-pass, dynamic flow exposure system (Figure 2-1). Particles are generated into diluting air and, when breathed, pass through one-way rebreathing valves at the mouthpiece; exhaled particles and excess aerosol are removed via an exhaust system. Particles are continuously generated, and the exposure concentration is monitored and regulated during the exposure. All tubing is electrically conductive with lengths minimized to avoid particle loss. Dilution air is filtered through charcoal and high-efficiency particle air filters. Particle mass in the intake diluting air is undetectable, with numbers ranging from 0 to 10 particles/cm^3. After generation, particles pass through a charge neutralizer to achieve Boltzman's equilibrium. The ionized particles then enter a 28.4 L mixing reservoir. Particles in the reservoir enter the circuitry to the mouthpiece according to the demands of the subject. An overflow line exhausts the excess aerosol. Non-rebreathing valves at the mouthpiece ensure one-way passage of the particles and allow aerosol concentrations to be analyzed in real time on both the inspiratory and the expiratory sides of the subject. The particle size at the mouth of the generator was essentially identical to that measured at the mouthpiece. The residence time of the particles in the mixing chamber was very brief (120 L/min in a 28.4 L chamber). This was verified by checking the particle number at several points in the inspiratory line. There was essentially no agglomeration after the particles exited the generator.

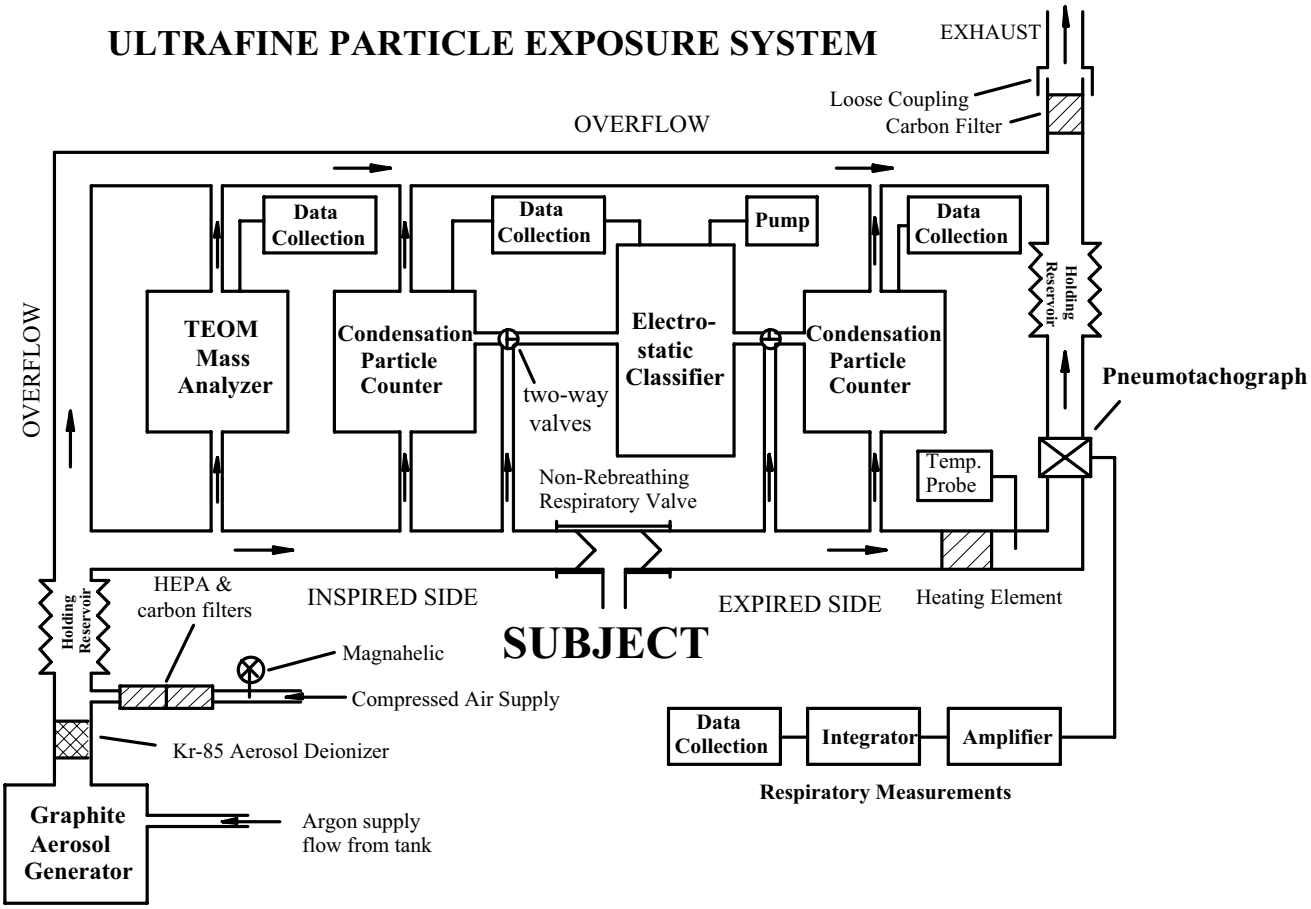

Figure 2-1. Ultrafine particle generation and exposure system. "Subject" indicates the position of the volunteer being exposed, breathing through a mouthpiece. The non-rebreathing valves direct airflow in a single pass from the holding reservoir on the inspiratory side toward the expiratory holding reservoir and exhaust. Positions of monitoring equipment and ports are indicated; see Table 1 for equipment sources.

The intake airflow rate must be sufficient to meet instantaneous demands of the subject under a variety of conditions. Minute ventilation at rest is typically 6 to 8 L/min but increases several fold with exercise. Instantaneous or peak flow rates can reach 100 L/min. To meet peak demands of the subject, the flow rate into the mixing chamber on the inspiratory side of the system is 120 L/min. A resilient reservoir is placed on the expired side of the subject, which is loosely coupled to a dedicated filter and exhaust system. The system is designed to keep both sides of the non-rebreathing valves at atmospheric pressure, unaffected by the subject's respiration. The intake supply flow rate is monitored with a Magnahelic pressure gauge (Dwyer Instruments, Inc., Michigan City, IN) calibrated using a dry test meter (Singer American Meter Company Division, Wellesley, MA).

Tubing on the expiratory side can be heated to ~37°C to avoid condensation from possible supersaturation accompanying cooling of water-saturated air from human breath. A pneumotachograph provides a respired airflow signal that is electronically integrated to obtain volumetric data. Table 2-1 lists the instrumentation used for generation and monitoring of UFP in this system.

Table 2-1. Equipment for the ultrafine particle exposure facility.

Item	*Manufacturer*
Ultrafine Graphite Generator	Palas GmbH, Karlsruhe, Germany
TEOM Mass Balance	Rupprecht and Patashnick, Albany, NY
Condensation Particle Counter (2)	TSI, Inc., St. Paul, MN
Electrostatic Classifier	TSI, Inc., St. Paul, MN
Non-rebreathing Valve (2)	Hans Rudolph Inc., Kansas City, MO
Pneumotachograph	E for M Co., White Plains, NY
HPChem Integrating Software	Hewlett Packard, MD

Calibration: The CPC and Electrostatic Classifier are calibrated by TSI. The Pneumotachograph is calibrated with a Medical Graphics (St. Paul, MN) syringe before each exposure. The TEOM is compared with filter samples during each exposure.

PARTICLE GENERATION

In our system, ultrafine particles are generated in the Palas generator by spark discharge between two electrodes in an anhydrous argon atmosphere. Argon serves to exclude oxygen, water vapor, and other gases to minimize the formation of organic compounds and oxidation products. For initial studies and validation of this exposure system, the electrodes consisted of pure graphite (Palas Company, Germany). The particle size distribution is determined by varying both the gap between the electrodes and the spark frequency. The generator continually adjusts the electrode position to keep the gap, and therefore the particle size, constant during particle generation. A constant flow (6 L/min) of argon through the spark chamber during generation minimizes particle agglomeration. Following generation, particles are diluted with filtered air in the mixing chamber to the desired particle concentration. The mass and number concentrations of UFP emitted from the Palas generator were found to be very stable over time. For example, over a period of 2 hours, with a target number concentration of 2×10^6 particles/cm^3, the actual mean ± SD particle number was $2.07 \pm 0.07 \times 10^6$. The details of the exposure system and particle generation and characterization have been recently published (10).

PARTICLE CHARACTERIZATION

Particle characterization is accomplished by determination of particle mass, number concentration, and size distributions. Mass concentration is measured using the tapered element oscillating microbalance (TEOM), which measures the mass collected on an exchangeable filter cartridge by monitoring the corresponding frequency changes of a tapered element. This technology is certified by the U.S. Environmental Protection Agency for continuous monitoring of PM_{10} and $PM_{2.5}$. The equipment can be calibrated for mass and flow measurements to National Institute of Standards and Technology traceable standards. The TEOM provides mass concentrations in $\mu g/m^3$ at averaging times of 1 minute to 24 hours, with lower limits of mass determination on the order of 5 $\mu g/m^3$. The TEOM mass balance is sensitive to pressure changes within the system; these are controlled by the system design. At the low mass concentrations planned for human clinical studies of UFP (e.g., 10 to 50 $\mu g/m^3$), relatively long averaging times of several hours are required to provide accurate mass determinations. For this reason, we determined a standard curve of particle mass versus number concentration to validate TEOM mass measurements with estimates based on particle number. The mass concentration is monitored continuously on the inspired limb of the system, but we rely on real-time monitoring of particle number to ensure constant levels of particle generation during exposures.

The UFP number concentration is determined using a condensation particle counter. This technology enlarges the particles by heterogeneous condensation so that they are large enough to be counted optically. The counter can detect particle sizes ranging from 10 nm to 3 µm, at concentrations ranging from approximately 0.01 to 1 x 10^7 particle/cm^3. Our exposure system utilizes counters on both the inspiratory and the expiratory sides of the subject so that we can monitor particle number concentrations simultaneously.

The particle size distribution is determined using the electrical differential mobility analyzer. Particles are separated into specific size ranges according to their ability to traverse an electrical field. The differential mobility analyzer and the condensation particle counter along with the controlling software constitute a scanning mobility particle system, which provides particle number concentration, surface area, and volume (mass) concentration as a function of particle diameter. The system is capable of classifying particles with electrical mobility diameters in the range of 5 to 1,000 nm.

Size characterization of the carbon UFP produced using the Palas generator is shown in Figure 2-2. Using an output of 10% of full scale on the low voltage setting and a spark frequency of 30/sec, the geometric mean particle size by number was 25.7 nm, geometric standard deviation (GSD) 1.64. The number and mass histograms showed similar size distributions.

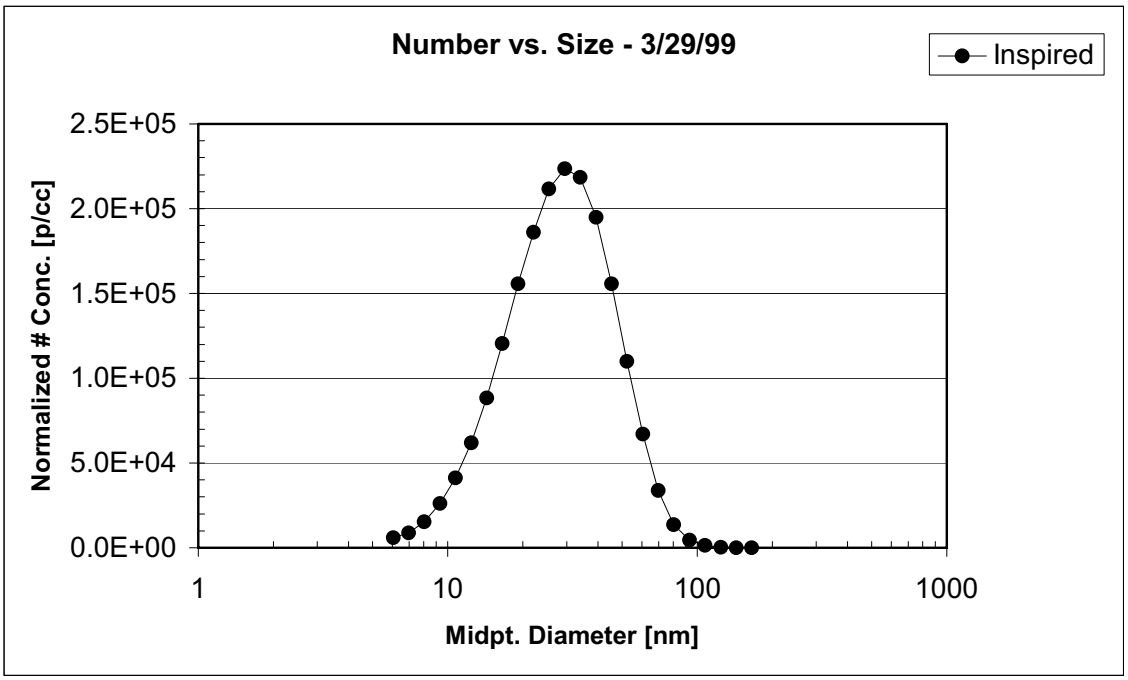

Figure 2-2. Size distribution, by number, of ultrafine carbon particles generated for inhalation.

PARTICLE COMPOSITION

While conducting these studies, we learned from colleagues in Germany (Dr. G. Oberdörster, personal communication) that ultrafine carbon particles generated for their studies, using a Palas generator similar to ours, contained a substantial fraction of organic carbon (up to 25%). We considered the following possible sources for the organic material: 1) adsorption of organic materials from the air after collection of the particles; 2) trace impurities within the argon gas supply (the argon is 99.998% pure); and 3) contaminating sources within the generation system. The graphite rods used to generate the particles are heated to a very high temperature prior to use, which would eliminate any contaminating organic materials. We undertook efforts to identify and eliminate any potential sources of organic material in the exposure system itself.

Closer examination of the Palas generation system indicated several potential sources for the organic carbon material on the particles. One was the internal combustion chamber, which is made of black plastic; another was the black plastic collars holding the graphite electrodes, which come into contact with the argon flow perfusing the combustion chamber. In addition, there are several flexible plastic tubes inside the generator that transport the incoming argon flow to the inner combustion chamber and diluting air to the exit of that chamber. We replaced these parts one by one with Teflon® (inner combustion chamber), ceramic (collar piece), or corrugated stainless steel tubing (inner tubes). A further potential source for the off-gassing of organic components was the plastic tubing between the argon tank and the generator, which

initially consisted of PET tubing. This, too, was replaced by metal tubing (copper). Essentially, the whole exposure system was rebuilt to eliminate sources of organic contamination. Following these modifications, measurements confirmed that ultrafine carbon particles generated in the Palas combustion chamber had less than 1% organics.

Subsequent analyses of particles collected from the modified Palas generator revealed that the content of organic carbon was insignificant, generally less than 10% by mass. We suspect the remaining small amount of organic carbon may represent adsorption of organic carbon from the diluting air after particle generation. To test this possibility, we utilized a new technique for single-particle analysis of composition developed by Dr. Kim Prather and colleagues (11), using aerosol time-of-flight mass spectrometry (ATOFMS). Dr. Prather found that UFP analyzed immediately after emissions from the rebuilt generator were predominantly elemental carbon. The single-particle mass spectra of the UFP were nearly identical to those of elemental carbon particles from gasoline- and diesel-powered emissions sources measured previously: 82% of the particles showed short-chain fragment patterns of C1, C2 and C3; 14% showed longer-chain fragmented peaks. Thus, 96% of the particles consisted of elemental carbon (Dr. K. Prather, personal communication). We performed validation and characterization studies confirming that the operating characteristics of the generator and size distribution of the particles generated were not altered by the modifications made to the generator. We therefore concluded that subjects' inhaled particles consisted of elemental carbon and that these were similar in composition to ambient elemental carbon particles.

SYSTEM LOSSES

Accurate determination of particle deposition requires correction for particle losses within the exposure system. We determined particle losses, in terms of both mass and number, at conditions of varying airflow simulating rest and exercise, and for various particle sizes within the range of the generated particles. A reciprocal pump was used to simulate respiration. A resting minute ventilation of 10 L/min was simulated using a volume of 800 ml at 12.5 cycles/min. Mild exercise (22 L/min) was simulated using a volume of 1,200 ml at 18.3 cycles/min. Continuous upstream and downstream measurements of particle number and volume were determined for the whole system and for a respiratory valve alone. Mass losses were calculated using particle volume determined by the electrostatic classifier.

In this system, losses attributable to the tubing and the mixing reservoir were negligible; the majority of losses occurred on the two silicone valves that control direction of airflow. The total mean particle loss for each valve was 8.2% by number and 6.4% by mass. As expected, losses were greater for smaller particles and with slower flow rates. The average fractional losses for the system as a whole, at ventilation rates of 10 and 22 L/min, are shown in Table 2-2. In correcting for valve losses during actual exposures, losses due to the upstream valve are subtracted from the measured inspired concentrations, and the downstream valve losses are added to the expired concentrations.

Table 2-2. Particle losses in the exposure system.

Count median particle diameter (nm)	*Particle loss (%) 10 L/min*	*Particle loss (%) 22 L/min*
7.5	13.2	3.9
13.3	8.4	1.1
23.7	6.0	0
42.2	6.4	0
75.0	4.7	0
133.4	0.0	0
Total system losses*	8.2	0.8

*Losses for all particles, not mean of values for each size range. See text for method of determination

RESPIRATORY MEASUREMENTS

Particle deposition is influenced by changes in respiratory flow rates, breathing frequency, and tidal volume. The mouthpiece exposure system permits real-time monitoring of these parameters using a pneumotachograph on the expiratory side of the subject. Airflow signals from the pneumotachograph are electronically integrated to provide volumetric data, which are displayed on a computer screen during exposure. Data are analyzed to provide average minute ventilation, respiratory rate, and tidal volume both at rest and during exercise. These data are used, along with particle mass and number concentrations, to determine particle intake and deposition for each subject.

Other variables that are monitored and controlled during exposures include temperature, relative humidity, and oxygen concentration of both the air delivered to the subject and the ambient air within the room housing the exposure facility. Relative humidity and temperature can have significant effects on particle delivery as well as measurement. The inspired air temperature is maintained at ~27°C.

Section 3

EXPOSURE PROTOCOL AND PARTICLE DEPOSITION (TASK 2)

This project involved three clinical exposure studies to ultrafine particles of carbon; the results of the first two studies were reported in the interim report but are summarized here to allow comparisons. The first involved 12 subjects (6 female) exposed at rest to 10 $\mu g/m^3$ UFP or filtered air for 2 hours. Exposures were separated by at least two weeks, blinded to both subjects and investigators, and the order randomized. The second involved 12 subjects (6 female) with three exposures for each subject, with exposures separated by at least two weeks: 10 $\mu g/m^3$ UFP, 25 $\mu g/m^3$ UFP, and filtered air. For safety reasons, the order of exposure was randomized in a restricted fashion, such that each subject received the 10 $\mu g/m^3$ exposure before the 25. To simulate outdoor activities, subjects exercised on a bicycle ergometer for 15 minutes of each half-hour at an intensity adjusted to increase the minute ventilation to approximately 20 $L/min/m^2$ body surface area.

The experimental protocol for these studies is summarized in Figure 3-1. The studies required five to seven visits for each subject. Visit 1 was a screening day. Informed consent was obtained, and subjects completed a standardized questionnaire for assessment of respiratory symptoms, medical history, and smoking history. A physical examination was performed, followed by routine pulmonary function tests, consisting of spirometry, diffusing capacity, and measurement of lung volumes. Subjects exercised on the bicycle ergometer for 15 minutes to determine the intensity necessary to achieve a minute ventilation of 20

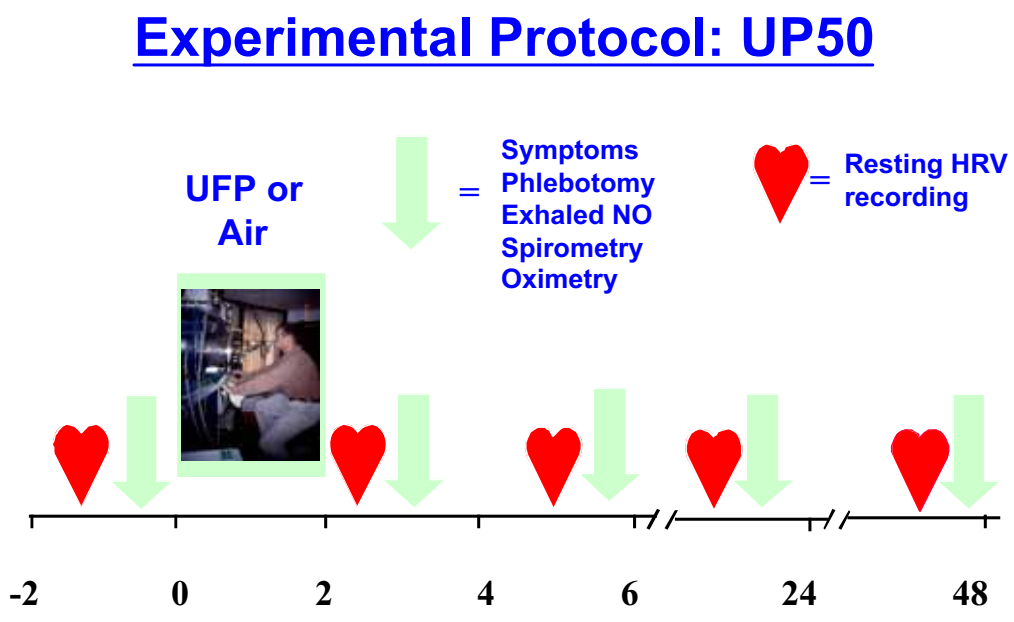

Figure 3-1. Experimental protocol for the clinical studies; the 50 $\mu g/m^3$ study included monitoring for 48 hours after exposure.

L/min/m^2. For females, pregnancy testing was performed. Finally, subjects underwent sputum induction by inhaling nebulized saline (see below).

On Visit 2, at least one week after the screening day, subjects arrived at 7:15 A.M. for the following: blood pressure, heart rate, pulse oximetry, symptom questionnaire, attachment of a 12-lead Holter heart monitor with a resting recording for 10 minutes, phlebotomy, measurements of exhaled nitric oxide (NO), and spirometry. These procedures required about 2 hours. Subjects were then exposed by mouthpiece for 2 hours to either filtered air or UFP, with intermittent exercise. Subjects breathed room air through the mouthpiece for 5 minutes before the exposure was actually started. A 10-minute break from the mouthpiece was taken after 1 hour of exposure.

Immediately after the exposure, the preexposure measurements were repeated. The subject then was provided lunch and remained in the Clinical Research Center. Identical measurements were taken 3.5 hours after exposure, and the subject was discharged with an activity diary.

On Visit 3, subjects returned the next morning at 8:00 A.M. The series of measurements were again performed, and sputum induced. Finally, the Holter monitor was removed. Subjects then returned for subsequent exposure at least 2 weeks after exposure, using an identical protocol.

The third protocol involved exposures of 16 subjects (8 male and 8 female) to 50 ug/m^3 UFP versus air for 2 hours with intermittent exercise as described above. Exposures were now separated by at least 3 weeks. Respiratory symptoms, blood pressure, heart rate, pulse oximetry, and phlebotomy were performed before, immediately after, and 3.5 and 21 hours after exposure. Digital, 12-lead high-resolution electrocardiogram (ECG) recordings were performed at each time-point before and after exposure, and 48-hour ambulatory cardiac monitoring was initiated at the start of exposure. In addition, because of our earlier observations of small declines in oxygen saturation in females, subjects underwent continuous digital pulse oximetry monitoring throughout the postexposure period and overnight at home. For this protocol, subjects returned for a final series of measurements 45 hours after exposure (Visit 4). Although pulmonary function studies were not routinely measured in this protocol, the diffusing capacity for carbon monoxide (DL_{CO}) was measured immediately before and 21 and 45 hours after exposure.

A total of 40 volunteer subjects were enrolled in these protocols, 20 female and 20 male. All were lifetime nonsmokers aged 18–52 years. All had normal baseline pulmonary function tests, a normal 12-lead EKG, and no history of chronic respiratory disease. Two subjects were Asian, one African American, and the rest white. The study was approved by the Institutional Review Board for Research Subjects of the University of Rochester Medical Center, and all subjects provided written, informed consent.

Section 4

BIOLOGIC ENDPOINTS (TASKS 3 AND 4)

PULMONARY FUNCTION

Spirometric measurements of forced vital capacity and forced expiratory volume (FEV_1) were performed with a pneumotachograph interfaced with a microcomputer (Model CPF-S, Medical Graphics, St. Paul, MN). Lung volumes (by plethysmography) and DL_{CO} were measured in the clinical pulmonary function laboratory using equipment from Morgan Scientific Inc., Haverhill, MA.

Airway Nitric Oxide

Measurement of airway nitric oxide (NO) production provides a noninvasive method for assessing airway inflammation (1). We have developed methods for separately measuring NO production in the conducting (or upper) airways ($\dot{V}_{UNO}$), and NO production in the alveolar (or lower) airways ($\dot{V}_{LNO}$) (12,13). The technique involves determination of the single-breath diffusing capacity for NO (DL_{NO}) (14) and measurement of the partial pressure of exhaled NO (PE) at differing constant expiratory flow rates. During all measurements, exhalation against positive pressure closed the nasopharyngeal vellum and thus prevented contamination of the expired airway gases with NO from the nasopharynx.

Nitric oxide concentrations in the exhaled breath were measured with a rapidly responding chemiluminescence NO analyzer (model 270B, Sievers, Boulder, CO) operating at a sampling rate of 250 ml/min. The analyzer was calibrated daily using serial dilutions of a gas containing 229 ppb NO. Reference gas samples free of NO (zero air) were obtained by passing compressed air from a cylinder containing less than 2 ppb of NO (Scott Specialty Gases, Plumsteadville, PA) through a filter packed with potassium permanganate (Purafil, Thermoenvironmental Instruments, Franklin, MA). To correct for instrument drift, all measurements were corrected by subtracting the average of zero air readings taken immediately before and after each NO determination.

BLOOD MARKERS OF COAGULATION AND INFLAMMATION

Fibrinogen, Factor VII, and von Willebrand factor were analyzed in the laboratory of the Vascular Medicine Program, Orthopedic Hospital, Los Angeles, using standard assays. Venous blood was collected in sodium citrate anticoagulant, and the plasma was separated, aliquoted, and stored at –80°C prior to shipment. Interleukin-6, IL-8, serum amyloid A, soluble intercellular adhesion molecule-1 (ICAM-1), soluble L-selectin, P-selectin, and E-selectin were determined using commercial enzyme-linked immunosorbent assays that were validated using dilution and add-back experiments. For these assays,

venous blood was collected in heparin anticoagulant, and aliquots of plasma were stored as above prior to analysis.

BLOOD LEUKOCYTE IMMUNOFLUORESCENCE ANALYSIS

Flow cytometry provided a sensitive method for evaluating changes in cell differential counts and for assessing changes in phenotype and expression of activation markers and adhesion molecules on blood leukocytes. Our choice of cell surface molecules to be studied was based on the goal of delineating changes in lymphocyte subsets, cell activation, and expression of adhesion molecules, all of which may reflect responses to inflammation and endothelial activation.

Fresh heparinized whole blood was stained with fluorochrome-labeled monoclonal antibodies (Becton Dickinson, Mountain View, CA), with appropriate isotype control antibodies. Leukocytes were stained with the desired mAb conjugated to fluoroscein isothiocyanate (FITC) and simultaneously stained with both CD14-PE and CD45-PerCp (PerCp is a Becton Dickinson fluorochrome with minimal wavelength overlap with FITC or PE). This permitted determination of the relative expression of adhesion molecules and other markers separately on polymorphonuclear leukocytes, eosinophils, lymphocytes, and monocytes. Lymphocyte subsets were characterized using combination gating and selective markers: $CD3^+4^+$ (T-helper), $CD3^+8^+$ (T-cytotoxic-suppressor), $CD3^+$□□TCR^+ (T-null), $CD3^+19^+$ (natural killer), and $CD3^-$ $16/56^+$ (B cells).

Red blood cells were lysed and cells were analyzed on a FACScan™ flow cytometer (Becton Dickinson) equipped with a 15 mW argon ion laser at 488 nm. Ten thousand events were collected from each sample in list mode using Cell Quest software (Becton Dickinson). Parameters collected were forward scatter, 90° side scatter, and 3-color fluorescence (FITC; 530/30 nm band pass, PE; 585/42 nm band pass, and PerCP; 650 nm long pass filter). The appropriate isotype control antibodies were run with each experiment to assist in appropriate gate setting. Leukocyte subsets were determined as a percentage of gated cells and were multiplied by the concentration of leukocytes from the complete blood count to express subsets as concentrations of cells. Standardized fluorescent microbeads (Quantium 24P and 25P, Bangs Laboratories, Fishers, IN) were run with each experiment. These data were fitted with an exponential curve: $f(x) = Ae^{Bx}$ where x was the channel number and A and B were constants determined from the regression fit. The standard curve was then used to convert mean channel numbers for the various markers to molecules of equivalent soluble fluorochrome (15). This provided a correction for minor day-to-day instrument variations in fluorescence detection.

SPUTUM INDUCTION

The cells obtained in induced sputum are representative of the lower airways and provide a noninvasive measure of airway inflammation. Sputum induction was performed as part of baseline determinations on the screening day; subjects unable to produce an adequate sample ($\geq 0.7 \times 10^6$ cells with $\geq 70\%$ nonepithelial cells) were excluded from the study. Sputum was induced 22 hours after each exposure. Only one sputum induction was performed after each exposure because sputum induction itself induces a transient airway inflammatory response that influences repeated measurements (16,17). Sputum induction was modified from the method of Pizzichini (18). The cell-free supernatant was aliquoted and stored at –80°C for subsequent analysis of interleukin-6 and IL-8 using enzyme-linked immunosorbent assays.

CARDIAC MONITORING

The 12-lead Holter ECG was recorded digitally with commercial equipment (H-12, Mortara Instruments, Milwaukee, WI), according to the manufacturer's recommendations. At specified intervals during the recording (before exposure, immediately after exposure, 3.5 hours after exposure, 24 hours after exposure, and for the 50 $\mu g/m^3$ study, 48 hours after exposure), the subject reclined in a dark room and the recording was marked for detailed analysis of these segments. Detailed analysis was also performed during one exercise period during exposure and one segment of recording during sleep. The recordings were analyzed by the Cardiology Research Unit at the University of Rochester Medical Center. Conventional analyses of the incidence of supraventricular and ventricular ectopic beats, heart rate variability, and maximum S-T voltage elevation and depression were performed for each complete interval. Recordings from multihour intervals and the specific 5-minute quiet rest periods were analyzed to assess heart rate variability in the time and frequency domains, S-T voltage changes, and repolarization duration. This combination of analyses yielded information regarding autonomic nervous system effects (which might occur via direct reflexes from airways and/or inflammatory responses), myocardial vulnerability to arrhythmia, and the underlying state of health of the myocardial substrate (19).

CALCULATION OF PARTICLE DEPOSITION

Calculation of total respiratory particle deposition utilizes the following measurements: average inspiratory and expiratory number concentration and particle size distribution, and inspiratory mass concentration. These data are corrected for valve losses over the range of particle size. To keep calculations manageable, size data are arbitrarily grouped into six bins spanning the entire range of particle size; Table 2-2 shows the median diameter for each bin.

The deposition fraction (DF) was calculated in the following manner. One-hour averages were taken of the measured inspiratory and expiratory number concentrations. These total concentrations were multiplied by

the fraction of particles in each size bin to determine size-specific inspiratory and expiratory particle concentrations. Since system losses can occur across the rubber valves, we measured the losses across one valve and then applied the correction to both the inspired and the expired valves. Size-specific system losses were determined by multiplying the fraction of particles in each bin by the previously determined fractional loss (Table 2-2). These correction factors were then subtracted from the inspired concentrations and added to the expired concentrations. DF was then calculated as follows, using the corrected values:

DF = (inspiratory concentration – expiratory concentration) / inspiratory concentration.

For determination of the mass deposition fraction, we relied on scanning mobility particle system data on particle volume to indicate differences between inspiratory and expiratory particle mass concentrations, since direct mass measurements with the TEOM required long collection times at these low particle concentrations, and real-time expired mass measurements were therefore not sufficiently accurate with this instrument. The ratio of the 1-hour mean inspired volume concentration to the expired volume concentration was multiplied by the inspired mass concentration to determine the expired mass concentration. DF by mass was then calculated in the same manner as for the number concentration.

STATISTICAL METHODS

The initial studies utilized a standard, two-period crossover design in which each subject received both particles and air. Equal numbers of males and females were included, since there was a possibility that some effects of particle exposure might be sex dependent. The order of presentation was randomized separately for each sex, with half of each group of subjects receiving each of the two possible orders. Between the two exposures was a washout period of sufficient duration that carryover effects from the first period to the second were expected to be minimal or nonexistent. The standard analysis for continuous endpoints is a repeated measures analysis of variance (ANOVA). In this analysis, order of presentation and sex are between-subjects factors, and treatment, period, and time (when there are repeated measurements after each exposure) are within-subject factors.

The second set of studies utilized a three-period crossover design in which each subject received air and both low (10 $\mu g/m^3$) and high (25 $\mu g/m^3$) levels of particles. For safety reasons, each subject received the low level of exposure before the higher one. There were then three possible exposure sequences, depending on where in the sequence the air exposure was placed. Equal numbers of subjects were randomly assigned to each sequence. The statistical analysis was based on the usual analysis of variance model for crossover designs (20). The final study with 50 $\mu g/m^3$ levels of particles used an identical analysis as the initial set of studies.

Section 5

RESULTS

PARTICLE CONCENTRATIONS IN THE RESEARCH ENVIRONMENT

We felt it was important to know numbers and mass concentrations of particles within the Clinical Research Center and the environmental chamber where the facility is located, as well as in the intake air for the exposure facility. The intake air for the exposures comes from the compressed air source for the hospital and is passed through a charcoal and a Fluoropore filter prior to entering the exposure system. For reference purposes, outdoor air above a construction site just outside the hospital was also sampled. We measured fine particle number (3 μm and smaller), ultrafine particle size distribution (0.1 μm and smaller), and total suspended particulate mass in these locations. Mass and number concentrations were run continuously in each location over a period of 70 to 110 hours.

Mean ± SD particle number concentrations were $3.63 \pm 1.15 \times 10^3$ particles/cm^3 in the Clinical Research Center, $5.86 \pm 2.11 \times 10^2$ particles/cm^3 in the environmental chamber, and $3.05 \pm 6.65 \times 10^4$ particles/cm^3 outside the hospital. Particle number in the Clinical Research Center was almost completely attributable to ultrafine particles ($3.56 \pm 1.93 \times 10^3$ particles/cm^3). In the Clinical Research Center, outside the environmental chamber, particle number and mass declined steadily during the evening hours when the unit was less active, with particle number reaching a low of 1.15×10^3 particles/cm^3. The highest peaks in particle number (2.78×10^4 particles/cm^3) were reached in the morning hours and coincided with intensity of activity on the unit. Outdoor fine particle numbers above the construction site were highly variable, and peaks exceeded 1.7×10^5 particles/cm^3. Particles were essentially undetectable in the filtered intake air for the mouthpiece exposure system.

PARTICLE DEPOSITION (TASK 2)

Brownian diffusion becomes increasingly important as a mechanism for deposition of particles increasingly smaller than 0.5 μm. Diffusional deposition should be maximal in the distal airways and alveoli because airway diameter is small and airflow is low, maximizing residence time. Therefore, respiratory deposition of UFP would be expected to be higher than for larger particles.

The objective of these studies was to assess the deposition of a polydisperse carbonaceous UFP aerosol in healthy human subjects at rest and during exercise. We hypothesized that the total respiratory deposition of UFP increases with decreasing particle size in the ultrafine range (< 0.1 μm) and that deposition increases further with exercise. The increase in respiratory deposition during exercise could be in part related to the

increased minute ventilation and possibly the increased flow demands during exercise, which would move the turbulence-to-laminar flow transition point distally, to smaller generation airways, enhancing deposition in those airways where laminar flow becomes turbulent (21). We also hypothesized that deposition would not differ by sex during spontaneous breathing.

Two sets of exposure studies were performed. All exposures were by mouthpiece for 2 hours, with a 10-minute break from the mouthpiece after the first hour. In the first set of exposures (Series 1), subjects (n = 12) were exposed to 10 $\mu g/m^3$ (~2 x 10^6 particles/cm^3) UFP at rest. In the second set of exposures (Series 2), subjects were exposed to 10 and 25 $\mu g/m^3$ (~7 x 10^6 particles/cm^3) UFP on separate occasions. Exposures included 15 minutes of moderate exercise (target minute ventilation 25 L/min/m^2 body surface area) on a bicycle ergometer, alternating with 15 minutes at rest, with a total of four exercise periods. In Series 2, data were available for only 7 of the 12 subjects for technical reasons. (We found in the first few subjects that measurements of expiratory particle concentrations were inaccurate because of pressure changes associated with the subject's breathing during exercise. Repositioning the expiratory sampling port resolved this problem). For subjects in Series 2 with usable data from both exposure concentrations, there was no significant difference in deposition measured at 10 $\mu g/m^3$ and 25 $\mu g/m^3$, and data were averaged. A manuscript describing the deposition of UFP from these studies has been accepted for publication (21).

Figure 5-1 shows the particle monitoring data from a typical subject exposure session. A healthy volunteer was exposed at rest for 2 hours (mean exposure mass concentration = 10.1 ± 2.1 $\mu g/m^3$), with a 10-minute break from the mouthpiece after 1 hour. The inspiratory particle number tracings are interrupted because the inspiratory condensation particle counter is switched to monitor expiratory particle numbers during particle size classification measurements; inspiratory particle size measurements are done without the subject, before the start of the exposure. Expiratory particle number concentration is lower than inspired, reflecting respiratory deposition primarily, as well as particle loss across the respiratory valves.

The age, sex, and mean spirometric values of the subjects for both studies are shown in Table 5-1. Table 5-2 shows the mean V_T, respiratory rate, and minute ventilation during the exposures. In Series 2, exercise led to a doubling of V_T and a 50% increase in respiratory rate, giving a more than threefold increase in minute ventilation.

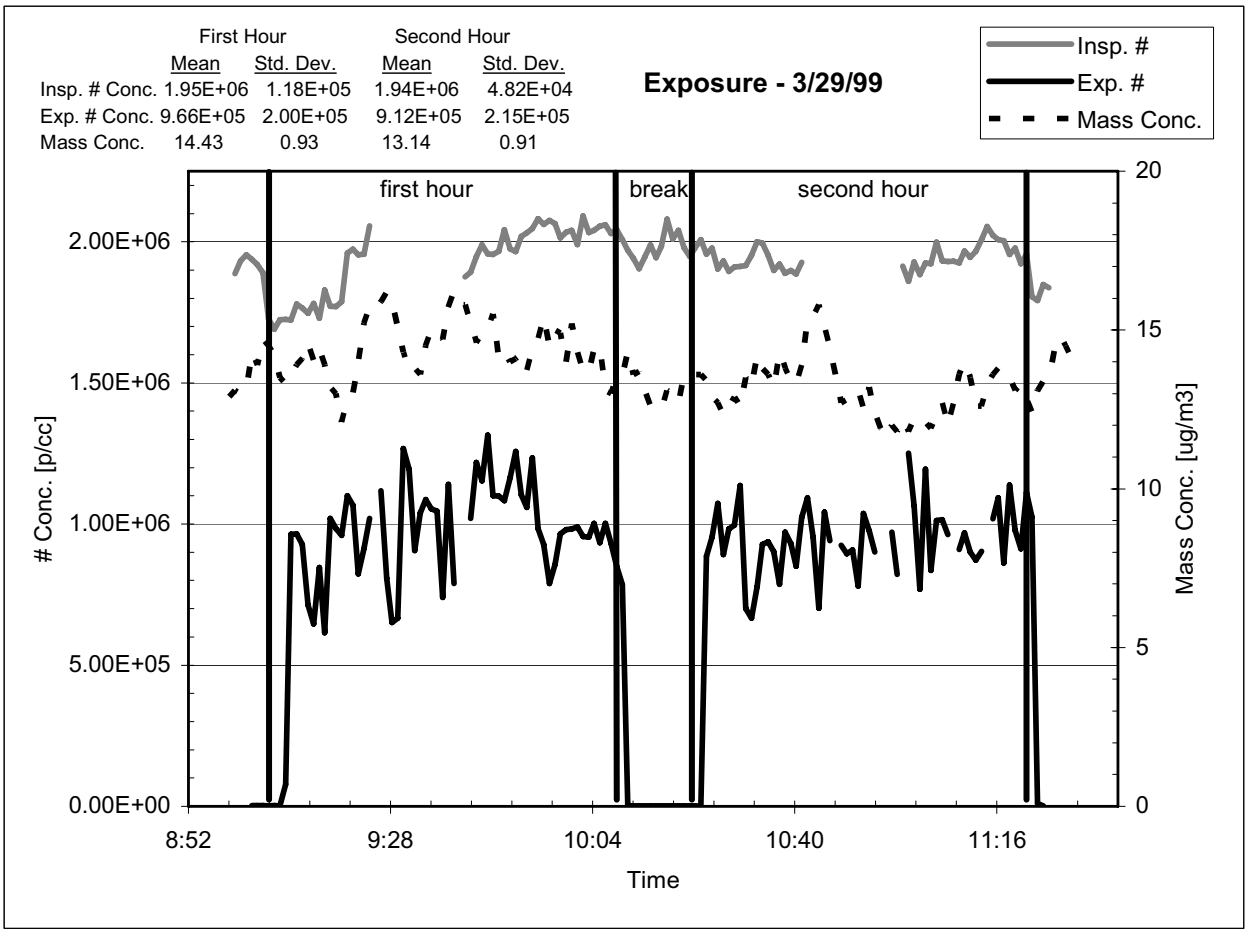

Figure 5-1. Typical results of real-time monitoring of mass and number concentrations during an exposure. The subject was exposed to approximately 10 µg/m^3 UFP for 2 hours with a 10-minute break after the first hour. Data are collected at 1-minute intervals. Data shown prior to correction for system losses.

Table 5-1. Subject demographics.

	Series 1 ***(n = 12)***	***Series 2*** ***(n = 7)***
Mean age (age range)	30 (18–52)	24 (18–33)
Male/female	6/6	5/2
FVC (L)*	4.13 ± 0.91	5.05 ± 1.16
FEV_1 (L)*	3.61 ± 0.70	4.38 ± 0.91
FEV_1/FVC*	0.88 ± 0.04	0.87 ± 0.06

*Mean ± SD.

Table 5-2. Breathing parameters*

	Subjects	*Tidal volume (L)*	*Respiratory rate (breaths/min)*	*Minute ventilation (L/min)*
Series 1 (rest)	12	0.58 ± 0.13	16 ± 2.8	9.0 ± 1.3
Series 2 (rest)	7	0.60 ± 0.11	20 ± 2.4	11.5 ± 2.3
Series 2 (exercise)	7	1.33 ± 0.35	29 ± 5.4	38.1 ± 9.5

*Data are means ± SD.

Table 5-3 shows the deposition data from Series 1 with the subjects at rest, including deposition by particle size. The highest deposition fraction was seen with the smallest particles. DF fell as particle size increased up to 48.70 nm and 64.94 nm, where it leveled off (Table 5-3). The total DF for the individual subjects ranged from 0.43 to 0.80 by particle number and 0.36 to 0.74 for mass (data not shown).

Table 5-3. Deposition fraction by particle size in 12 healthy subjects at rest (Series 1)

Midpoint diameter (nm)	*Deposition fraction (mean ± SD)*
8.7	0.80 (± 0.09)
11.6	0.78 (± 0.08)
15.4	0.74 (± 0.09)
20.5	0.70 (± 0.12)
27.4	0.66 (± 0.13)
36.5	0.59 (± 0.13)
48.7	0.55 (± 0.14)
64.9	0.55 (± 0.13)
Total DF by particle number	0.66 (± 0.12)
Total DF by particle mass	0.59 (± 0.13)

The deposition data for Series 2, at both rest and exercise, are shown in Table 5-4. The results at rest were similar to Series 1, and DF increased with exercise in all size bins. DF by particle size again plateaued in the larger size bins both at rest and with exercise (Table 5-4). The total number DF for the individual subjects ranged from 0.55 to 0.66 at rest and 0.76 to 0.88 with exercise.

No significant sex differences were found. In the first set of exposures with subjects at rest, the mean ± SD number DF was 0.68 ± 0.05 for men (n = 6) and 0.65 ± 0.05 for women (n = 6). The corresponding mass DFs were 0.60 ± 0.05 and 0.56 ± 0.05, respectively. There were not enough subjects in Series 2 to make sex comparisons.

Table 5-4. Deposition fraction (DF) in 7 healthy subjects at rest and exercise (Series 2)

Midpoint diameter (nm)	*DF at rest**	*DF during exercise**
8.7	0.74 (± 0.07)	0.94 (± 0.02)
11.6	0.74 (± 0.06)	0.91 (± 0.02)
15.4	0.68 (± 0.05)	0.89 (± 0.03)
20.5	0.63 (± 0.05)	0.84 (± 0.04)
27.4	0.60 (± 0.05)	0.79 (± 0.05)
36.5	0.58 (± 0.05)	0.75 (± 0.05)
48.7	0.58 (± 0.05)	0.72 (± 0.07)
64.9	0.67 (± 0.07)	0.72 (± 0.09)
Total DF by particle number	0.63 (± 0.04)	0.83 (± 0.04)
Total DF by particle mass	0.60 (± 0.05)	0.76 (± 0.06)

*Data are means ± SD.

BIOLOGICAL EFFECTS (TASKS 3 AND 4)

Exposures at Rest

Respiratory symptoms, spirometry, blood pressure, pulse oximetry, and exhaled NO were assessed before and at intervals after the exposure. Sputum induction was performed 18 hours after exposure. Continuous 24-hour, 12-lead Holter monitoring was performed on the day of the exposure and analyzed for arrhythmias, S-T segment changes, changes in heart rate and heart rate variability, and repolarization phenomenon.

Results of these studies have been published in abstract form (see Related Publications, below). There were no significant differences between air and UFP exposure at 10 $\mu g/m^3$ in respiratory symptoms, spirometry, blood pressure, pulse oximetry, exhaled NO, or sputum cell differential counts, using paired t-tests.

A repeated measures ANOVA has been completed on all of the endpoints in this study. There were very few significant treatment effects observed—no more than would be expected by chance alone. In addition, the grouping of treatment effects was not consistent with a priori hypotheses. Therefore, we concluded there were no significant health effects or physiological changes in response to breathing 10 $\mu g/m^3$ carbon UFP at rest.

Exposures with Exercise

Two exposure studies involving exercise were undertaken. In the first, 12 healthy subjects were exposed to air and to two concentrations of UFP, 10 and 25 $\mu g/m^3$, for 2 hours, with intermittent exercise on a bicycle ergometer. The second study examined effects of a higher UFP concentration, 50 $\mu g/m^3$, compared with air exposure in 16 healthy subjects. These combined studies provided an examination of exposure responses over a range of UFP concentrations from 0 to 50 $\mu g/m^3$. In addition, for the 50 $\mu g/m^3$ study, pulse oximetry was recorded continuously, and DLCO was added as an outcome measure.

Exposure to 10 and 25 $\mu g/m^3$ UFP. As in the resting study, there were no symptoms, changes in lung function, or evidence for airway inflammation (induced sputum or exhaled NO) associated with the exposures. Interestingly, pulse oximetry showed a small but statistically significant decrease in oxygen saturation in females after exposure to 25 $\mu g/m^3$ UFP (Figure 5-2; this and the following figures show change from preexposure measurement).

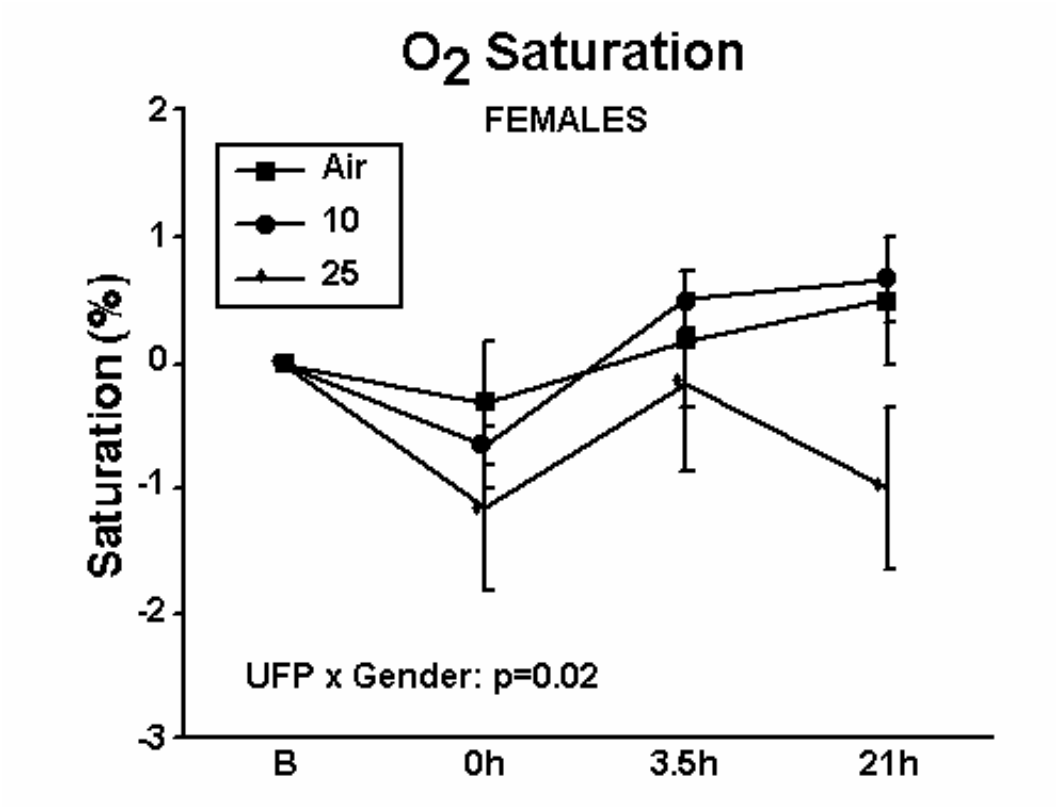

Figure 5-2. Hemoglobin-oxygen saturation by pulse oximetry in 6 females exposed to air and 10 and 25 μg/m^3 UFP. Data are means ± SE of differences from preexposure baseline (B). 0h refers to immediately postexposure.

In these studies, we examined quantitative surface expression of molecules that mediate leukocyte-endothelial interactions and serve as indirect indicators of exposure effects on pulmonary vascular endothelium. Measurements of lymphocyte subsets and their activation by UFP were selected to reflect relative priming of circulating leukocytes as a consequence of airway inflammation. Studies of blood leukocytes showed early reduction in blood monocyte expression of intercellular adhesion molecule-1 (ICAM-1, CD54) in both males and females (Figure 5-3), and later reductions in the percentage of blood monocytes in females (Figure 5-4) that were greatest 21 hours after exposure. There was no significant change in the total white count. There was increased lymphocyte expression of CD25 (an epitope of the IL-2 receptor, a marker of activation), again only in females (Figure 5-5). The reductions in leukocyte adhesion molecule expression seen in these studies suggest the possibility of leukocyte sequestration or margination in response to UFP.

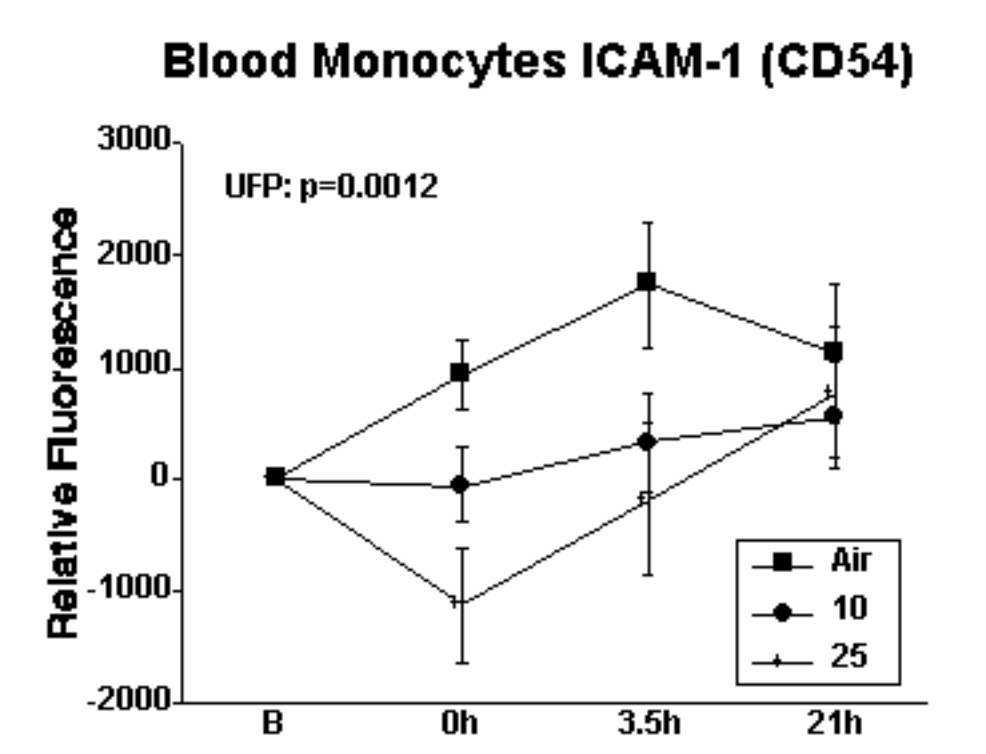

Figure 5-3. Expression of intercellular adhesion molecule-1 (ICAM-1, CD54) on blood monocytes, by multiparameter flow cytometry. Data are means ± SE of differences from preexposure baseline (B). 0h refers to immediately postexposure.

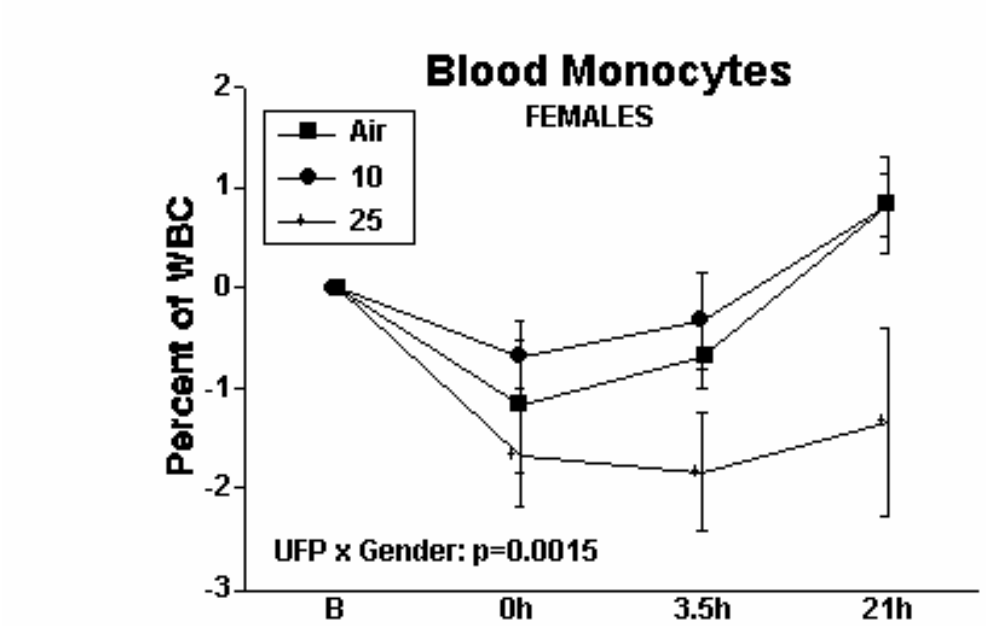

Figure 5-4. Percentage of blood monocytes from the leukocyte differential count. Data are means ± SE of differences from preexposure baseline (B). 0h refers to immediately postexposure.

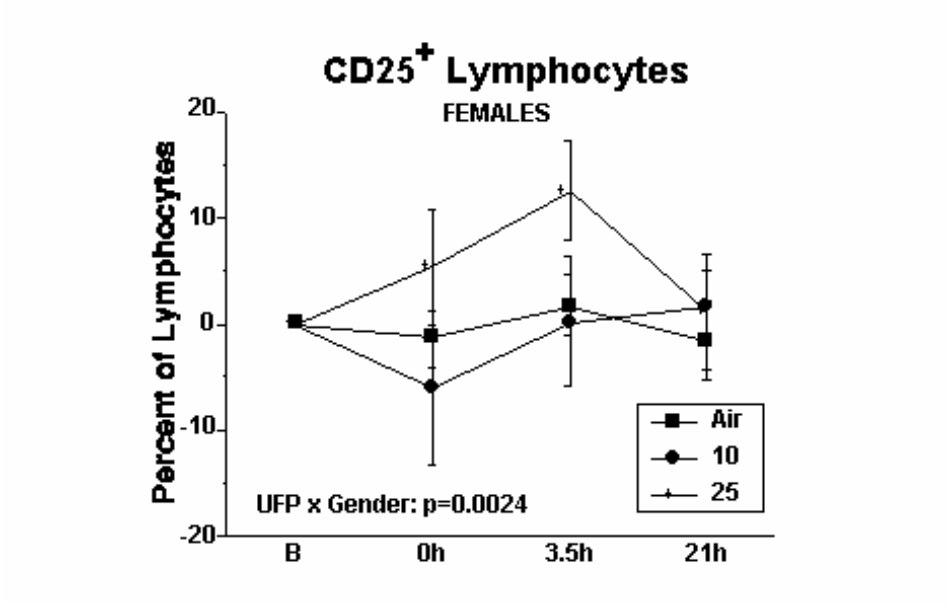

Figure 5-5. Expression of CD25 on blood lymphocytes, by multiparameter flow cytometry. Data are means ± SE of differences from preexposure baseline (B). 0h refers to immediately postexposure.

Analyses of cardiac monitoring included a detailed analysis of heart rate variability and repolarization intervals before exposure, during one of the exposure exercise periods, at time points after exposure, and during sleep. Exercise had profound effects on the ECG parameters recorded during exposure with pure air or UFP, with the ANOVA showing highly significant time-related effects for most of the parameters. Frequency-domain heart rate variability analysis indicated that the response of the parasympathetic system (measured by normalized units of high-frequency components) is slightly blunted during recovery from exercise immediately after exposure to UFP compared with pure air exposure (Figure 5-6). This diminished vagal response was not observed 3.5 hours later.

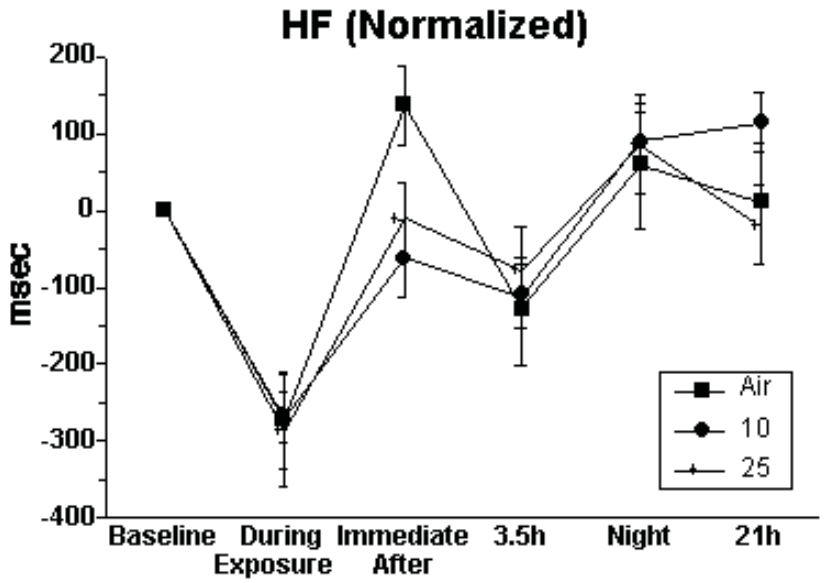

Figure 5-6. Changes in high-frequency component of heart rate variability. Five-minute segments of the ECG recording were analyzed at each indicated time point. For baseline, immediately after, and 3.5 and 21 hours after, subjects were supine in a darkened room. "During exposure" was during the final exercise period. Data are means ± SE of differences from preexposure baseline (B).

The analysis of QT interval duration and T-wave amplitude, conducted in the same healthy subjects, also showed a blunted response of repolarization duration after UFP exposure in comparison to pure air exposure. Figure 5-7 shows that QT shortened during exercise more substantially during UFP exposure than during pure air exposure and that the QT interval remained shortened for several hours after UFP exposure but not after pure air exposure. This blunted repolarization response could be seen in an exaggerated form when using Bazett's correction of QT for heart rate (QTc interval; Figure 5-8). Simultaneously, T-wave amplitude also was higher after exercise with UFP than after exercise with pure air (Figure 5-9). We did not observe these repolarization changes in subjects undergoing exposures in the first series of exposures at rest.

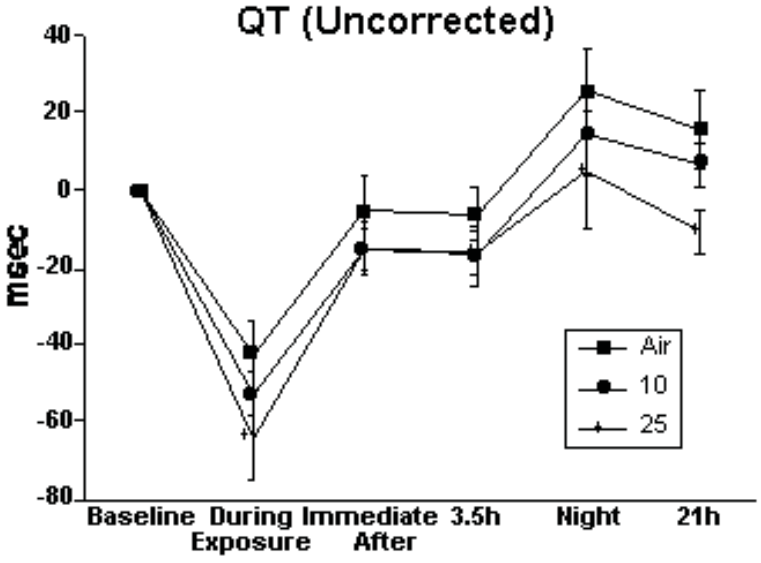

Figure 5-7. Changes in the QT interval (uncorrected) on the ECG recording. See legend for Figure 9.

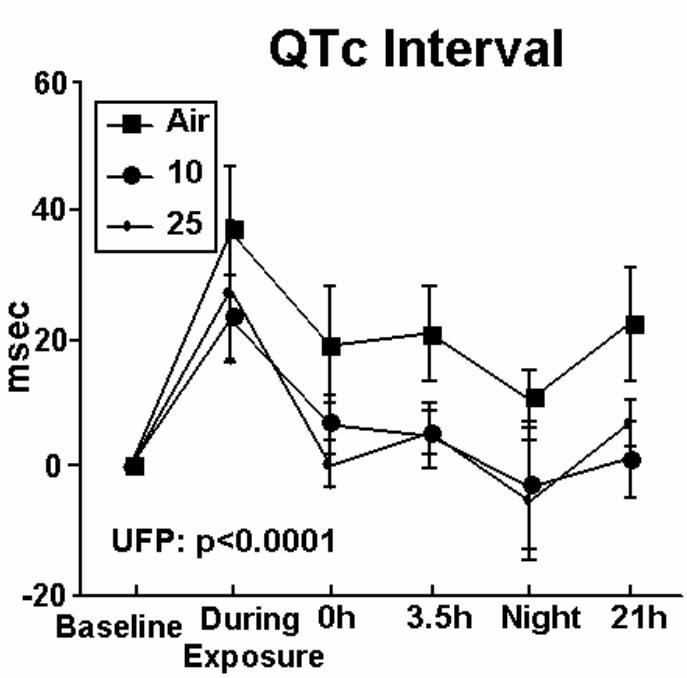

Figure 5-8. Changes in the QT interval, using Bazette's correction for heart rate. See legend for Figure 9. 0h refers to immediately postexposure.

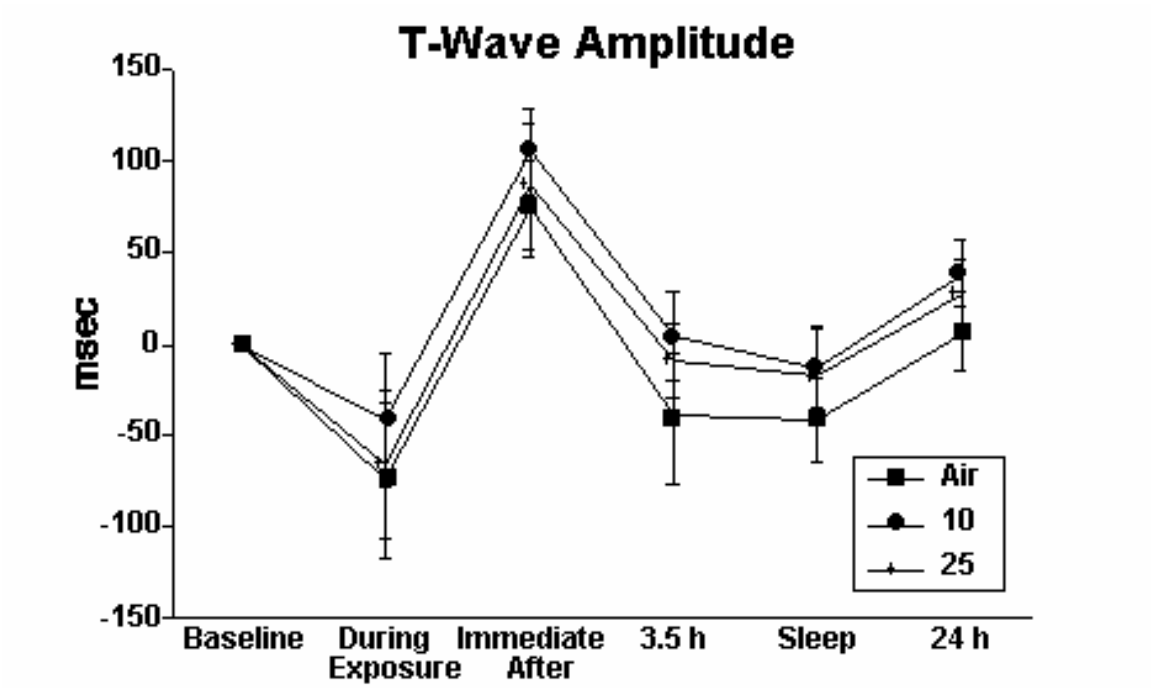

Figure 5-9. Changes in T-wave amplitude on the ECG recording. See legend for Figure 5-6.

There were no particle-related effects on symptoms, spirometry, airway nitric oxide production, or sputum cell differential counts. In other words, there was no evidence for induction of airways inflammation or irritant effects. There were also no increases in blood concentrations of fibrinogen, von Willebrand factor, or clotting Factor VII.

Exposure to 50 μg/m^3 UFP. Findings from this study confirmed that exposure to carbon UFP reduces leukocyte expression of adhesion molecules. There was a significant reduction in expression of CD18 on blood monocytes after exposure to 50 μg/m^3 UFP compared with air (Figure 5-10, $p < 0.001$). CD54 expression on monocytes also decreased with UFP exposure, as was seen with exposures to 10 and 25 μg/m^3. In this study, the reduction in CD54 expression was greater in males than in females (UFP x sex, $p = 0.025$). These reductions in leukocyte adhesion molecule expression together with the reduction in lymphocyte activation markers are similar to the findings seen with exposure to 25 μg/m^3, further supporting the possibility of leukocyte sequestration or margination in response to UFP. We observed a significant change in DL_{CO} 21 hours after exposure to 50 μg/m^3 UFP compared with air (change in DL_{CO} after UFP = –1.76 ± 0.66 ml/min/mmHg versus air = –0.18 ± 0.41 ml/min/mmHg, $p = 0.04$; Figure 5-11). This difference also disappeared when DL_{CO} was remeasured at 45 hours (change in DL_{CO} after UFP = –0.67 ± 0.0.65 ml/min/mmHg versus air = –0.54 ± 0.37 ml/min/mmHg, $p = 0.90$).

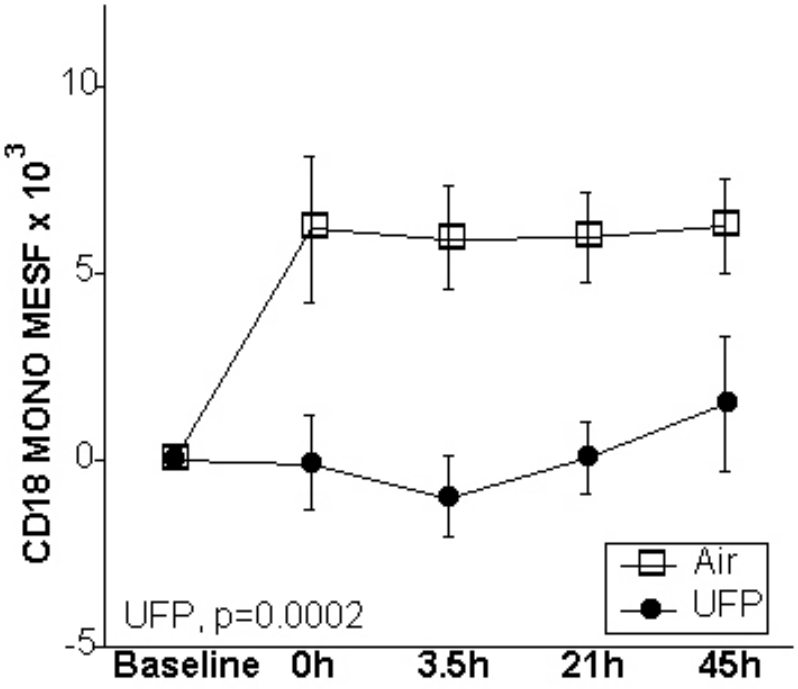

Figure 5-10. Change in monocyte expression of CD18 after exposure to 50 μg/m^3 carbon UFP. 0h refers to immediately postexposure.

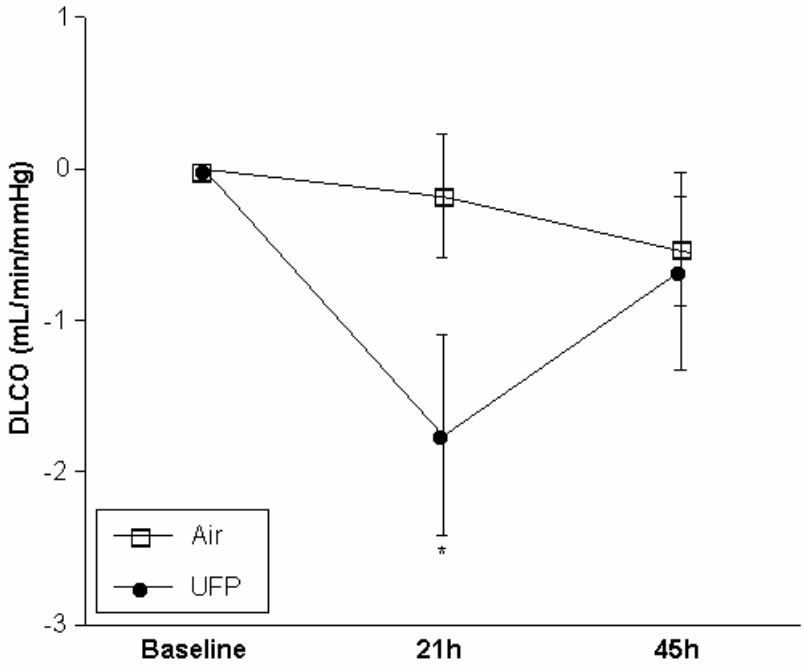

Figure 5-11. Change in DL_{CO} before and after exposure to filtered air vs. 50 µg/m^3 UFP. There was a significant decline in DL_{CO} 21 hours after exposure to 50 µg/m^3 UFP. This difference resolved when the measurement was repeated 45 hours after exposure. *p = 0.04 UFP versus filtered air.

Figure 5-12 shows the results for alveolar airway NO exchange parameters in the 50 µg/m^3 protocol. There was a trend toward a reduction in DL_{NO} after exposure to 50 µg/m^3 UFP, but this change did not achieve statistical significance. Changes in $\dot{V}_{LNO}$ and PA were significantly different after UFP exposure versus filtered air by ANOVA (UFP exposure x time, p = 0.030 and p = 0.039, respectively) but not by individual t-test comparisons at the various time points after exposure.

With regard to blood markers of inflammation and coagulation, there were no increases in clotting factors or in markers of the acute-phase response. Soluble L-selectin decreased in females 21 hours after exposure but increased in males (time x UFP x sex, p = 0.006). Markers of coagulation and thrombolysis were measured in the laboratory of Dr. Robert Devlin at the U.S. Environmental Protection Agency. Preliminary analysis shows no significant effects of UFP exposure on concentrations of D-dimer, plasminogen activator inhibitor-1, von Willebrand factor, plasminogen, fibrinogen, or Factor VII.

The ECG monitoring studies showed a statistically significant main effect of UFP exposure on the interval between normal QRS complexes (p = 0.048 by ANOVA). The normal-to-normal interval decreased (i.e., heart rate increased) during exposure with exercise, to a greater degree with UFP exposure than with air exposure (Figure 5-13), although the differences in heart rate were not clinically significant. The T-wave amplitude decreased following UFP exposure in females but not in males (UFP x sex, p = 0.042; figure not shown). Finally, there was a significant interaction between time, exposure, and sex for low-frequency heart rate variability, expressed as normalized units (p = 0.017). As shown in Figure5-14, males showed a

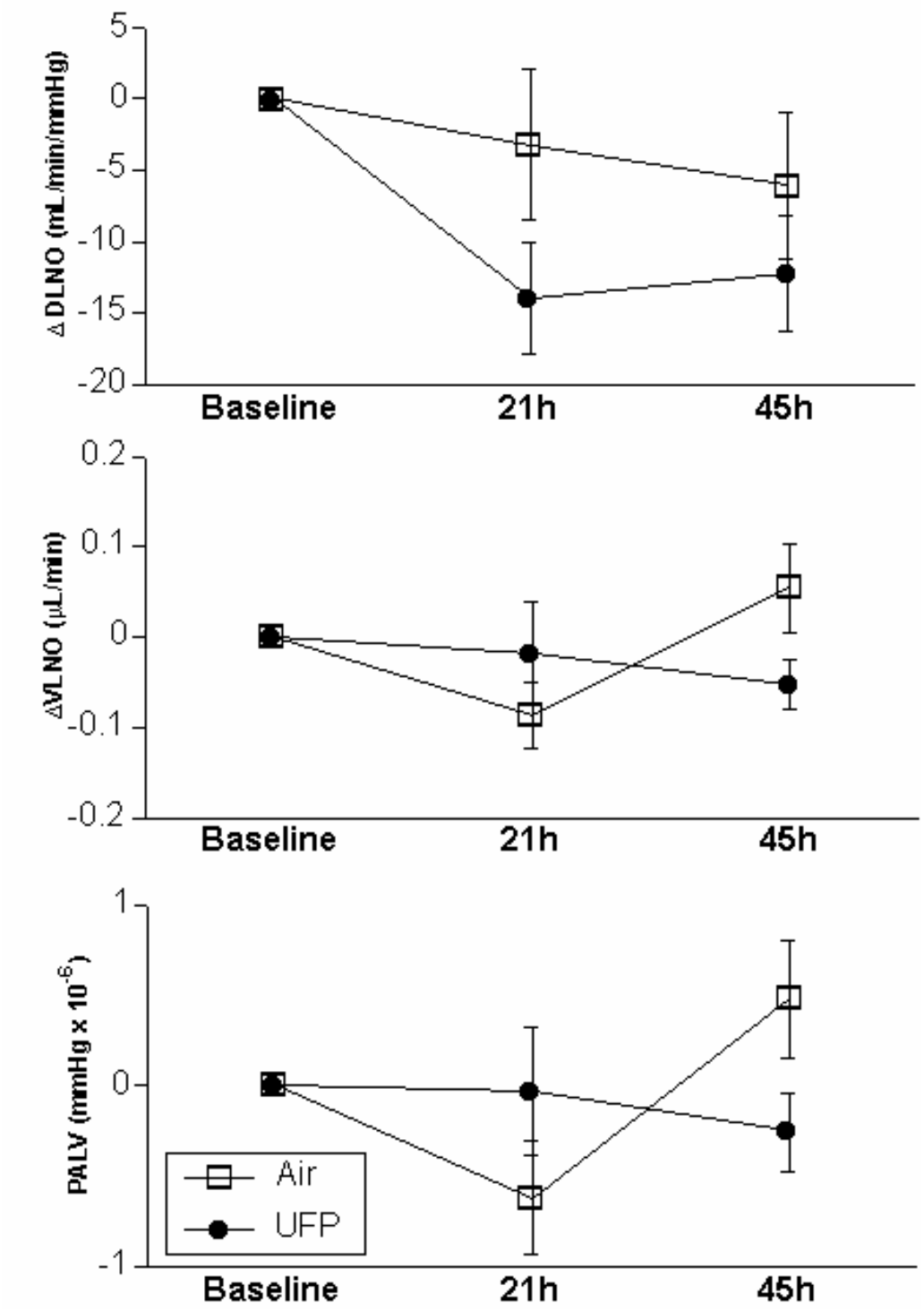

Figure 5-12. Change in alveolar airway NO parameters after exposure to filtered air versus UFP. DL_{NO} declined in normal subjects after exposure to 50 μg/m^3 UFP, but the difference was not statistically significant. Consistent patterns of change in $\dot{V}_{LNO}$ and PA were not detected, although the differences between exposures were statistically significant by ANOVA.

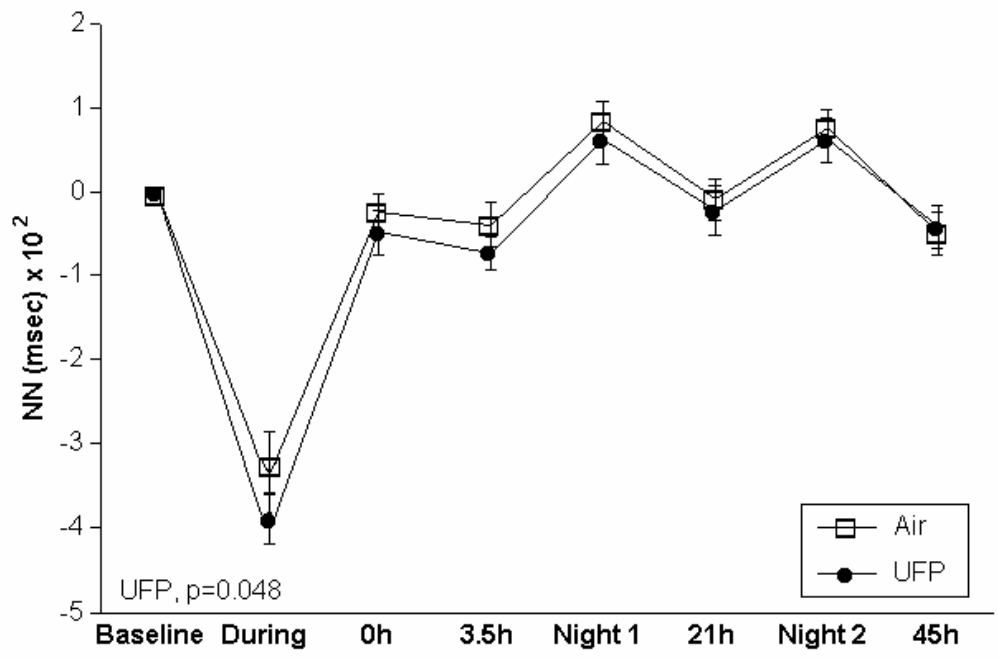

Figure 5-13. Change in cardiac normal-to-normal beat interval with exposure to air versus 50 μg/m^3 UFP.

transient but substantial reduction in low-frequency heart rate variability during exposure. This was not seen with females. There were no significant changes in the duration of myocardial repolarization.

There were no significant effects on oxygen saturation, as measured by continuous pulse oximetry, and no effects on symptoms.

To briefly summarize the clinical findings, inhalation of carbon UFP at concentrations up to 50 μg/m^3 caused no symptoms, changes in lung function, or evidence for airway inflammation in healthy subjects. Blood leukocyte subsets and adhesion molecules expression did reveal changes consistent with alteration of vascular endothelial function. We also found effects on the diffusing capacity, which decreases significantly 21 hours after exposure to UFP; diffusing capacity depends on pulmonary capillary blood volume and also reflects an effect on the pulmonary vascular system. Finally, we found effects on heart rate variability and on cardiac repolarization in healthy subjects. If confirmed, the findings that inhalation of UFP has cardiovascular effects would be highly relevant to our understanding of particle-induced health effects. (See details in Discussion, below.)

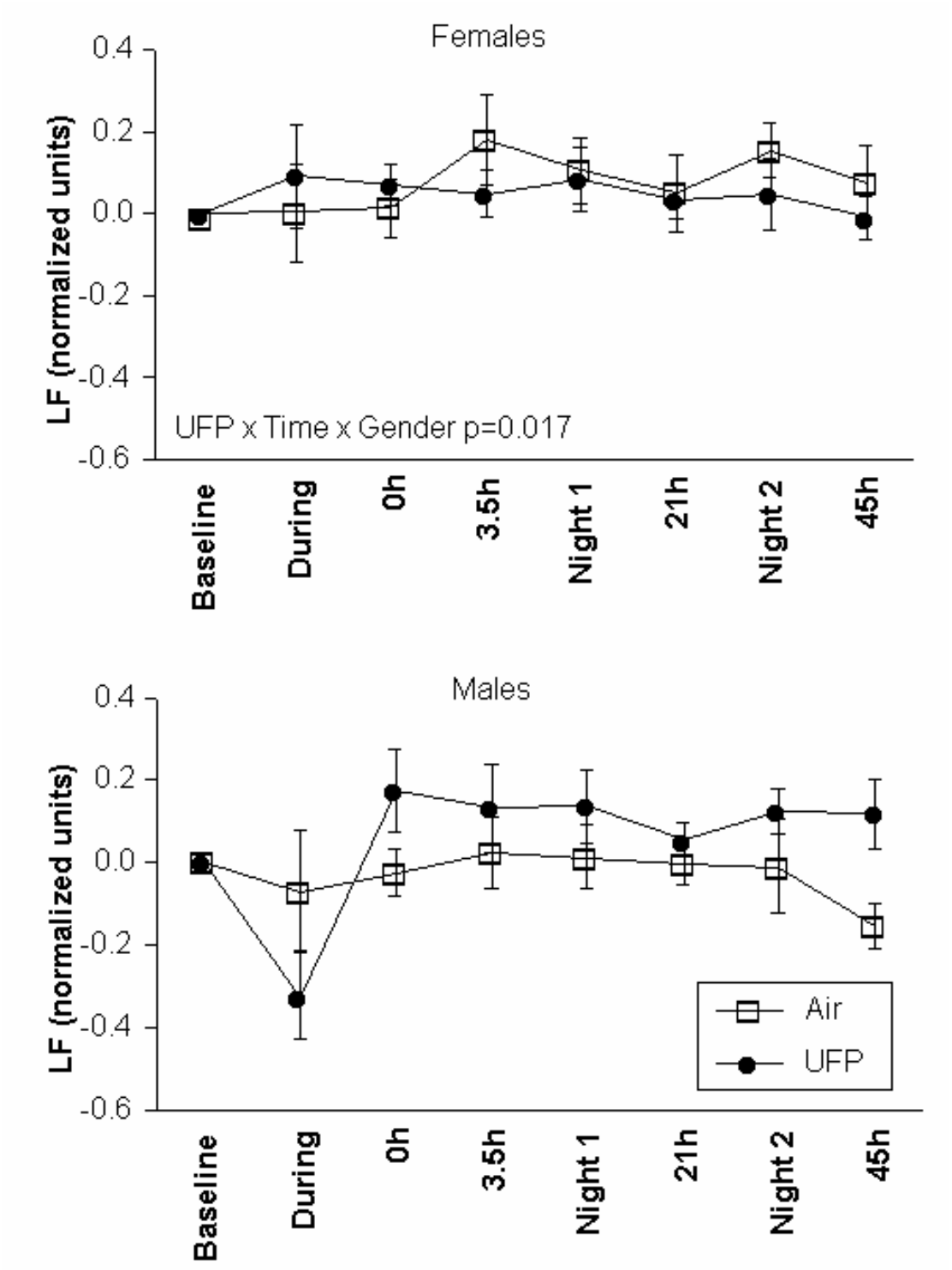

Figure 5-14. Change in low-frequency heart rate variability expressed as normalized units.

Section 6

DISCUSSION

The studies suggest that exposure to ultrafine particles at mass concentrations of 10–50 μg/m^3 may cause subclinical effects on pulmonary ventilation/perfusion matching, circulating leukocytes, and cardiac repolarization in healthy subjects, particularly in females. If these findings are confirmed, they will represent the most convincing support for the ultrafine hypothesis to date and suggest that females experience higher susceptibility to UFP exposure. Interestingly, our data did not confirm our original hypothesis, that ultrafine particle exposure with exercise would induce an acute-phase response.

Taken together, these findings are most consistent with particle effects on vascular endothelium, leading to subtle changes in pulmonary capillary perfusion, sequestration of monocytes that are expressing higher levels of CD54 (ICAM-1) and CD18 (leaving the low-expressing cells in the circulation), and shifts in circulating lymphocyte populations. The increased lymphocyte CD25 expression may represent mobilization of activated cells to the blood or, alternatively, sequestration of less activated cells in tissues. There is evidence that ultrafine particles enter the blood (2), and it is possible that there are direct effects of particles on circulating leukocytes in the blood. It is interesting that, in our previous studies, blood monocytes from healthy cigarette smokers expressed very low levels of ICAM-1 compared with nonsmokers (22,23). It is possible that we are seeing effects of UFP inhalation that are a subtle or transient version of what happens with inhalation of cigarette smoke, which is known to cause acute and chronic endothelial dysfunction. For example, acute exposure to cigarette smoke alters endothelial surface markers, resulting in release of mediators that attract cells to the endothelium, causing inflammation and injury; on a more chronic basis, cigarette smoking causes vascular plaque formation on the vascular surface and ultimately progression of atherosclerosis.

Our preliminary finding suggesting an effect of UFP on parasympathetic modulation of the heart is in agreement with observation by Gold et al. (24), who also found reduction in parasympathetic (vagal) tone in elderly Boston subjects exposed to ambient pollution levels with mean 4-hour $PM_{2.5}$ levels ranging from 3 to 49 μg/m^3. In our analysis, none of the time-domain heart rate variability parameters or low-frequency components showed significant changes induced by UFP.

The repolarization changes were seen with exposures to 10 and 25 μg/m^3 but not with 50 μg/m^3. It is possible that this effect does not follow the traditional concentration-response paradigm at higher concentrations, or that the initial observation was a chance occurrence. If there are significant effects of UFP exposure on repolarization, the mechanisms could be complex. A blunted response of vagal modulation on the sinus node does not fully explain the observed blunted response of QTc duration after UFP exposure. It is known that heart rate (sinus node function under the influence of the autonomic

nervous system) provides only a partial explanation for changes in QT duration (25). It is plausible that UFP impose an additional effect on repolarization either through a direct effect of the autonomic nervous system on ventricular myocardium (apart from that on the sinus node) (26) or by directly affecting ion channel function in ventricular myocardium through a yet-unknown mechanism.

Myocardial repolarization is governed by a complex interplay of numerous myocardial cell membrane ion channels (27). Many of these channels have been characterized and cloned, and there are known genetic abnormalities that impair ion channel function, prolonging repolarization, with increased susceptibility to arrhythmias and sudden death (28). Many conditions influence repolarization duration and morphology, including changes in heart rate, autonomic function, age, sex, many drugs, sleep, eating, smoking, diabetes, hypertension, and cardiac ischemia (29).

Generally, lengthening of the QTc interval predisposes to an increased potential for arrhythmias. However, shortening of repolarization is known to be caused by hypoxia and ischemia and to be arrhythmogenic (30). Calcium, potassium, and chloride channels may contribute significantly to shortening of the action potential duration. For example, the action potential shortening by chloride current activation may perpetuate reentry by shortening the refractory period (31,32). We saw only minimal reductions in O_2 saturation in our healthy female subjects; it is unlikely that this contributed significantly to the observed QT shortening, which did not show sex differences.

The other possible explanation for observed QT shortening may be the result of cardiac myocyte functional responses to subtle changes in systemic vascular tone, perhaps related to increased endothelin production and/or reduced NO release by endothelium in response to particles. Alternatively, UFP may gain access to pulmonary capillary blood, where they could be transported to the heart and cause direct effects on membrane ion channel function. Animal exposure studies are underway in Dr. Oberdörster's laboratory addressing this issue, and his preliminary data using inhalation of ^{13}C UFP indicate that UFP do reach other organs, including the liver, brain, and heart (33).

Evidence from other human studies indicates that exposure to concentrated ambient particles induces lung inflammation, systemic inflammatory responses, and vascular effects. Human studies of exposure to diesel exhaust at concentrations of 300 $\mu g/m^3$ have not shown acute effects on lung function but have shown distal airway inflammation and systemic hematological effects with increased white blood cell and platelet counts (34). In addition, expression of ICAM-1 was increased in vascular endothelium from bronchial biopsy specimens. Ghio and colleagues (35) found modest increases in polymorphonuclear neutrophils recovered in bronchoalveolar lavage fluid 24 hours after 2-hour exposures to concentrated ambient particles (at concentrations up to 311 $\mu g/m^3$). These investigators found an increased blood fibrinogen concentration in association with such exposure but no effects on symptoms, lung function, or blood leukocyte differential counts. Gong and colleagues (36) studied both healthy and asthmatic subjects exposed to

concentrated ambient particles at a concentration of 174 $\mu g/m^3$ with intermittent exercise. There were no effects on lung function and no evidence for airway inflammation in induced sputum. They did observe small increases in soluble-ICAM-1 at 4 and 24 hours after exposure and changes in heart rate variability consistent with enhanced parasympathetic influence on the heart. Clinical studies with concentrated ambient particles and diesel exhaust have generally been performed at concentrations that are nearly tenfold higher than our studies using ultrafine carbon particles.

It is difficult to compare the findings from those studies with our own, in part because of differences in the exposure atmospheres and in the endpoints being measured. The ambient particle concentrators used in those human studies do not concentrate ambient UFP; thus the exposure consisted of fine particles and ambient (unconcentrated) UFP. In addition, ambient PM represents a complex mixture of chemical species, including organic compounds and metals, which have been hypothesized to be important mediators of PM effects. In our studies, mass concentrations were approximately an order of magnitude lower than in the concentrated ambient particle studies, but particle number and surface area were likely higher. In addition, elemental UFP, by virtue of their large surface area, may carry an increased burden of reactive oxygen species compared with an equal mass of larger particles.

In our studies, the changes in response to ultrafine particles were small, but the subjects were young, generally healthy, nonsmoking adults. The brief duration of exposures may not have been sufficient to activate coagulation, lung function changes, or inflammatory pathways in healthy individuals. However, our findings do not exclude such processes in individuals with vascular disease risk factors or established cardiopulmonary disease, who may be more sensitive to low concentrations or brief UFP exposure. In addition, the limited sample sizes were likely inadequate to detect significant effects for some endpoints. This is particularly true for the comparisons between males and females.

Findings may differ for children, the elderly, or people with asthma or other chronic diseases. In complementary studies in asthmatics, we have observed that deposition of UFP is increased at rest and during exercise compared with healthy subjects (37). Indeed, people with severely compromised cardiovascular status may experience adverse effects from even small changes in vascular homeostasis. Furthermore, prolonged, repeated exposures may hasten the progression of atherosclerosis, as has been suggested by an epidemiologic study of fine particle exposure (38).

In summary, our data demonstrate that brief exposures to carbon UFP concentrations ranging from 10 to 50 $\mu g/m^3$ cause a range of cardiopulmonary responses. The effects were small, but the low concentrations and brief exposures may not have been adequate to provoke large or sustained effects in healthy volunteers, and carbon UFP lack many of the constituents, such as metals and organic species, believed responsible for adverse health effects. Furthermore, with our findings indicating possible effects of carbon UFP on vascular endothelium, an important next step is to examine these processes in individuals with vascular

disease risk factors or established cardiovascular disease. Our future studies will address cardiopulmonary responses to UFP using several different approaches: 1) we have extended our studies with carbon UFP to diabetics, a population with preexisting vascular disease; 2) we plan to initiate studies with concentrated ambient UFP comprising metals, organic species, and other constituents that may have adverse health effects; and 3) finally, we have initiated studies to look at the effects of inhaling ambient UFP in patients with coronary artery disease who are participating in an exercise program in a cardiac rehabilitation facility. Further clinical studies are needed to confirm our findings to date, determine their relationship to particulate matter size and composition, and investigate their mechanisms.

GLOSSARY

ANOVA	analysis of variance
DF	deposition fraction
DL_{CO}	diffusing capacity for carbon monoxide
DL_{NO}	diffusing capacity for nitric oxide
ECG	electrocardiogram
FITC	fluoroscein isothiocyanate
FEV_1	forced expiratory volume in 1 second
ICAM-1	intracellular adhesion molecule-1
NO	nitric oxide
PA	partial pressure of NO in the alveoli
PE	phycoerythrin
PM	particulate matter
$PM_{2.5}$	particulate matter < 2.5 μm in diameter
QT	interval from onset of ventricular polarization to the end of the T wave
QTc	QT interval corrected for heart rate using Bazett's formula
SD	standard deviation
SE	standard error
TEOM	tapered element oscillating microbalance
UFP	ultrafine particles (< 1 μm in diameter)
$\dot{V}_{LNO}$	NO production in alveolar airways
$\dot{V}_{UNO}$	NO production in conducting airways

RELATED PUBLICATIONS

MANUSCRIPTS (REPRINTS AVAILABLE UPON REQUEST)

Chalupa DF, Gibb FR, Morrow PE, Oberdörster G, Riesenfeld E, Gelein R, Utell MJ, Frampton MW. A facility for controlled human exposures to ultrafine particles. In: Heinrich U and Mohr U, Eds-in-chief: *Crucial issues in inhalation research—mechanistic, clinical and epidemiologic.* INIS Monographs, Fraunhofer IRB Verlag, Stuttgart, Germany, 2002.

Utell MJ, Frampton MW, Zareba W, Devlin RB, Cascio WE. Cardiovascular effects associated with air pollution: Potential mechanisms and methods of testing. *Inhalation Toxicol* 14:1231–1247, 2002.

Daigle CC, Chalupa DC, Gibb FR, Morrow PE, Oberdörster G, Utell MJ, Frampton MW. Ultrafine particles deposition in humans during rest and exercise. *Inhalation Toxicol* 15:539–552, 2003.

Pietropaoli AP, Frampton MW, Hyde RW, Morrow PE, Oberdörster G, Cox C, Speers DM, Frasier LM, Chalupa DC, Huang L-S, Utell MJ. Pulmonary function, diffusing capacity and inflammation in healthy and asthmatic subjects exposed to ultrafine particles. *Inhalation Toxicol* 16 (Suppl. 1): 59–72, 2004.

Pietropaoli AP, Frampton MW, Oberdörster G, Cox C, Huang L, Marder V, Utell MJ. Blood markers of coagulation and inflammation in healthy subjects exposed to carbon ultrafine particles. In: *Effects of air contaminants on the respiratory tract—interpretations from molecular to meta analysis*. INIS Monographs, Fraunhofer IRB Verlag, Stuttgart, Germany, 2004, pp.181–194.

Frampton, MW, Stewart J, Oberdörster G, Morrow PE, Chalupa D, Frasier LM, Speers DM, Cox C, Huang L-S, Utell MJ. Inhalation of ultrafine particles alters blood leukocyte expression of adhesion molecules in humans. *Environ Health Persp*, in press.

PUBLISHED ABSTRACTS

Boscia JA, Chalupa D, Utell MJ, Zareba W, Konecki JA, Morrow PE, Gibb FR, Oberdörster G, Azadniv M, Frasier LM, Speers DM, Frampton MW. Airway and cardiovascular effects of inhaled ultrafine carbon particles in resting healthy nonsmoking adults *Am J Respir Crit Care Med* 161:A239, 2000.

Frampton MW, Chalupa D, Morrow PE, Gibb FR, Oberdörster G, Boscia J, Speers DM, Utell MJ. Deposition of inhaled ultrafine carbon particles in resting healthy nonsmoking adults. *Am J Respir Crit Care Med* 161:A257, 2000.

Frampton MW, Azadniv M, Chalupa D, Morrow PE, Gibb FR, Oberdörster G, Boscia J, Speers DM, Utell MJ. Blood leukocyte expression of LFA-1 and ICAM-1 after inhalation of ultrafine carbon particles. *Am J Respir Crit Care Med* 163:A264, 2001.

Daigle CC, Speers DM, Chalupa D, Stewart JC, Frasier LM, Azadniv M, Phipps RP, Utell MJ, Frampton MW. Ultrafine particle exposure alters expression of CD40 ligand (CD154) in healthy subjects and subjects with asthma. *Am J Respir Crit Care Med* 165:A214, 2002.

Frampton MW, Zareba W, Daigle CC, Oberdörster G, Utell MJ. Inhalation of ultrafine particles alters myocardial repolarization in humans. *Am J Respir Crit Care Med* 165:B16, 2002.

Frampton MW, Stewart JC, Oberdörster G, Pietropaoli AP, Morrow PE, Chalupa D, Speers DM, Utell MJ. Inhalation of carbon ultrafine particles decreases expression of CD18 and CD11a on blood leukocytes. *Am J Respir Crit Care Med,* 169:A220, 2004.

Petronaci C-L, Pietropaoli AP, Utell MJ, Hyde RW, Morrow PE, Oberdörster G, Cox C, Speers DM, Frasier LM, Chalupa DC, Huang L-S, Frampton MW. Diffusing capacity, airway nitric oxide production, and pulmonary function in healthy subjects exposed to ultrafine carbon particles. *Am J Respir Crit Care Med.* 169:A281, 2004.

Pietropaoli AP, Delehanty JM, Perkins PT, Utell MJ, Oberdörster G, Hyde RW, Frasier LM, Speers DM, Chalupa DC, Frampton MW. Venous nitrate, nitrite, and forearm blood flow after carbon ultrafine particle exposure in healthy human subjects. *Am J Respir Crit Care Med.* 169:A883, 2004a.

REFERENCES

1. Oberdorster G, Gelein RM, Ferin J, Weiss B. Association of particulate air pollution and mortality: Involvement of ultrafine particles? *Inhal Toxicol* 1995; 7:111–124.

2. Nemmar A, Hoet PH, Vanquickenborne B, Dinsdale D, Thomeer M, Hoylaerts MF, Vanbilloen H, Mortelmans L,Nemery B. Passage of inhaled particles into the blood circulation in humans. *Circulation* 2002; 105:411–414.

3. Peters A, Wichmann HE, Tuch T, Heinrich J, Heyder J. Respiratory effects are associated with the number of ultrafine particles. *Am J Respir Crit Care Med* 1997; 155; 1376–1383.

4. Jeong C-H, Hopke PK, Chalupa, D, Utell M. Characteristics of nucleation and growth events of ultrafine particles measured in Rochester, NY. *Environ Sci & Technol* 2004; 38 (No.7): 1933–1940.

5. Tuch TH, Brand P, Wichmann HE, Heyder J. Variation of particle number and mass concentration in various size ranges of ambient aerosols in Eastern Germany. *Atmos Environ* 1997; 31(24): 4193–4197.

6. Brand P, Ruob K, Gebhart J. Performance of a mobile aerosol spectrometer for an in situ characterization of environmental aerosols in Frankfurt City. *Atmos Environ* 1992; 26A: 2451–2457.

7. Kittelson DB, Watts WF, Johnson JP. Mn/DOT Report No. 2001-12: Minnesota Department of Transportation 2001.

8. Elder A., Gelein, R, Finkelstein J, Phipps R, Frampton M, Utell M, Topham D, Kittelson D, Watts W, Hopke P, Jeong, C-H, Kim E, Liu W, Zhao W, Zhou L, Vincent R, Kumarathasan P, Oberdörster G. On-road exposure to highway aerosols. 2. Exposures of aged, compromised Rats. *Inhal Toxicol* 2004; 16(Suppl.1): 41–53.

9. Elder A, Corson N, Mercer P, Gelein R, Finkelstein J, Hopke P, Watts W, Kittelson D, Oberdörster G. Effects of on-road aerosols in aged rats. *Toxicologist* 2005; 84(S-1): 443.

10. Chalupa DF, Gibb FR, Morrow PE, Oberdörster G, Riesenfeld E, Gelein R, Utell MJ, Frampton MW. A facility for controlled human exposures to ultrafine particles. In: Heinrich U and Mohr U, Eds-in-chief: *Crucial issues in inhalation research—mechanistic, clinical and epidemiologic.* INIS Monographs, Fraunhofer IRB Verlag, Stuttgart, Germany, 2002.

11. Su YX, Sipin MF, Furutani H., Prather KA. Development and characterization of an ATOFMS with increased detection efficiency. *Analytical Chemistry* 2004; 76:712.

12. Hyde RW, Geigel EJ, Olszowka AJ, Krasney JA, Forster RE II, Utell MJ, Frampton MW. Determination of production of nitric oxide by the lower airways of humans—theory. *J Appl Physiol* 82:1290–1296, 1997.

13. Pietropaoli AP, Perillo IB, Torres A, Perkins PT, Frasier LM, Utell MJ, Frampton MW, Hyde RW. Simultaneous measurement of nitric oxide production by conducting and alveolar airways of humans. *J Appl Physiol* 87:1532–1542, 1999.

14. Perillo IB, Hyde RW, Olszowka AJ, Pietropaoli AP, Frasier LM, Torres A, Perkins PT, Forster RE II, Utell MJ, Frampton MW. Chemiluminescent measurements of nitric oxide pulmonary diffusing capacity and alveolar production in humans. *J Appl Physiol* 91:1931–1940, 2001.

15. Gavras JB, Frampton MW, Ryan DH, Levy PC, Cox C, Morrow PE, Utell MJ. Expression of membrane antigens on human alveolar macrophages after exposure to nitrogen dioxide. *Inhalation Toxicol* 6:633–646, 1994.

16. Nightingale JA, Rogers DF, Barnes PJ. Effects of repeated sputum induction on cell counts in normal volunteers. *Thorax* 53:87–90, 1998.

17. Holz O, Richter K, Jorres RA, Speckin P, Mucke M, Magnussen H. Changes in sputum composition between two inductions performed on consecutive days. *Thorax* 53:83–86, 1997.

18. Pizzichini E, Pizzichini MMM, Efthimiadis A, Hargreave FE, Dolovich J. Measurement of inflammatory indices in induced sputum: Effects of selection of sputum to minimize salivary contamination. *European Respiratory Journal* 9:1174–1180, 1996.

19. Zareba W, Nomura A, Couderc JP. Cardiovascular effects of air pollution: What to measure in ECG? *Environmental Health Perspectives* 109(supplement 4): 533–538, 2001.

20. Jones B, Kenward MG. Design and analysis of cross-over trials, New York, NY: Chapman and Hall: 1989.

21. Daigle CC, Chalupa DC, Gibb FR, Morrow PE, Oberdörster G, Utell MJ, Frampton MW. Particles deposition in humans during rest and exercise. *Inhal Toxicol* 2003; 15(6): 539–552.

22. Azadniv M, Torres A, Boscia J, Frasier L, Speers DM, Chow M, Utell MJ, Frampton MW. Blood leukocyte expression of adhesion molecules is altered in smoking and in mild asthma [abstract]. *Am J Respir Crit Care Med* 1999; 159:A109.

23. Frampton MW, Hyde RW, Torres A, Perillo I, Pietropaoli A, O'Mara R, Azadniv M, Frasier L, Speers D, Smith C, Utell MJ. Lung injury and inflammation in smokers: Effects of switching to a "new" cigarette [abstract]. *J Europ Respir Society* 2000;

24. Gold DR, Litonjua A, Schwartz J, Lovett E, Larson A, Nearing B, Allen G, Verrier M, Cherry R, Verrier R. Ambient pollution and heart rate variability. *Circulation* 2000; 101:1267–1273.

25. Davey P, Bateman J. Heart rate and catecholamine contribution to QT interval shortening on exercise. *Clin Cardiol* 1999; 22:513–518.

26. Merri M, Alberti M, Moss AJ. Dynamic analysis of ventricular repolarization duration from 24-hour Holter recordings. *IEEE Trans Biomed Eng* 1993; 40:1219–1225.

27. Tristani-Firouzi M, Chen J, Mitcheson JS, Sanguinetti MC. Molecular biology of K(+) channels and their role in cardiac arrhythmias. [Review] [71 refs]. *Am J Med* 2001; 110:50–59.

28. Zareba W, Moss AJ, Schwartz PJ, Vincent GM, Robinson JL, Priori SG, Benhorin J, Locati EH, Towbin JA, Keating MT, Lehmann MH, Hall WJ. Influence of the genotype on the clinical course of the long-QT syndrome. *N Engl J Med* 1998; 339:960–965.

29. Garson AJ. How to measure the QT interval—what is normal? *Am J Cardiol* 1993; 72:14B–16B.

30. Kimura S, Bassett AL, Furukawa T, Furukawa N, Myerburg RJ. Differences in the effect of metabolic inhibition on action potentials and calcium currents in endocardial and epicardial cells. *Circulation* 1991; 84:768–777.

31. Hiraoka M, Kawano S, HIrano Y, Furukawa T. Role of cardiac chloride currents in changes in action potential characteristics and arrhythmias. *Cardiovasc Res* 1998; 40:23–33.

32. Ruiz PE, Ponce ZA, Scanne OF. Early action potential shortening in hypoxic hearts: Role of chloride current(s) mediated by catecholamine release. *J Mol Cell Cardiol* 1996; 28:279–290.

33. Oberdörster G, Sharp Z, Atudorei V, Elder, A, Gelein R, Kreyling W, Cox C. Translocation of inhaled ultrafine particles to the brain. *Inhal Toxicol* 2004; 16 (6-7): 437–445.

34. Salvi M, Blomberg A, Rudell B, Kelly F, Sandstrom T, Holgate ST, Frew A. Acute inflammatory responses in the airways and peripheral blood after short-term exposure to diesel exhaust in healthy human volunteers. *Am J Respir Crit Care Med* 1999; 159:702–709.

35. Ghio AJ, Kim C, Devlin RB. Concentrated ambient air particles induce mild pulmonary inflammation in healthy human volunteers. *Am J Respir Crit Care Med* 2000; 162:981–988.

36. Gong H Jr, Linn WS, Sioutas C, Terrell SL, Clark KW, Anderson KR, Terrell LL. Controlled exposures of healthy and asthmatic volunteers to concentrated ambient fine particles in Los Angeles. *Inhal Toxicol* 2003; 15:305–325.

37. Chalupa DC, Morrow PE, Oberdörster G, Utell MJ, Frampton MW. Ultrafine particle deposition in subjects with asthma. *Environ Health Perspect* 2004; 112 (8): 879–882.

38. Kunzli N, Jerrett M, Mack WJ, Beckerman B, LaBree L, Gilliland F, Thomas D, Peters J, Hodis HN. Ambient air pollution and atherosclerosis in Los Angeles. *Environ Health Perspect* 2005; 113:201–206.

For information on other
NYSERDA reports, contact:

New York State Energy Research
and Development Authority
17 Columbia Circle
Albany, New York 12203-6399

toll free: 1 (866) NYSERDA
local: (518) 862-1090
fax: (518) 862-1091

info@nyserda.org
www.nyserda.org

Clinical Studies of Exposure to Ultrafine Particles

Final Report 05-11

State of New York
George E. Pataki, Governor

New York State Energy Research and Development Authority
Vincent A. DeIorio, Esq., Chairman
Peter R. Smith, President and Chief Executive Officer

NYSERDA